PANGEA
European Master in Paleontology, Geoheritage, Applications
Erasmus Mundus Joint Master Degree

With the support of the Erasmus+ Programme of the European Union

The Late Ordovician Glaciation in theVilluercas-Ibores-Jara Geopark: Sedimentology, Petrography, and Geosites Assessments

Abdullahi Aminu Alameen

UMinho | 2025

Universidade do Minho
Escola de Ciências

Abdullahi Aminu Alameen

The Late Ordovician Glaciation in the Villuercas-Ibores-Jara Geopark: Sedimentology, Petrography, and Geosites Assessment

julho de 2025

Universidade do Minho
Escola de Ciências

Abdullahi Aminu Alameen

The Late Ordovician Glaciation in the Villuercas-Ibores-Jara Geopark: Sedimentology, Petrography, and Geosites Assessment

Dissertação de Mestrado
Mestrado em Geociências
Área de especialização em Património Geológico e Geoconservação

Trabalho efetuado sob a orientação de
Doutor Diamantino Manuel Insua Pereira
Doutor Rolf Sören Jensen

julho de 2025

DIREITOS DE AUTORE CONDIÇÕES DE UTILIZAÇÃO DO TRABALHO POR TERCEIROS

ACKNOWLEDGMENTS

I sincerely thank my advisor, Professor Sören Jensen, for his continuous interest, encouragement, and generous advice throughout the entirety of this study. His exhibited patience and support have shaped me not only academically and professionally, but personally as well. Many thanks are also attributed to Professor Diamantino Pereira for his guidance and advice. Many thanks to Professor (retired) Teodoro Palacios Medrano, who accompanied Professor Sören Jensen and me during the fieldwork sessions, where he served as an invaluable resource for regional geology and local geography. Dr. Iván Cortijo and Andrey Nicolas Campos also served as esteemed guides during the fieldwork for the Charco de la Trucha geosite. I appreciate the support and opportunity provided by the Villuercas-Ibores-Jara UNESCO Global Geopark for this study.

This study would not have been possible without the financial assistance from Erasmus Mundus PANGEA. I would like to express my gratitude for the financial assistance provided through the scholarship, which enabled me to carry out this research. The support offered not only covered the essential academic and living expenses but also made it possible for me to focus fully on the completion of my thesis. I am deeply thankful for the opportunity to be part of this esteemed program, which has significantly enriched my academic journey and personal growth.

I am grateful to the universities of Lille, the University of Minho, and the National Kapodistrian University of Athens for providing such a valuable and enriching academic experience. Throughout this journey, I was fortunate to learn from erudite professors and work alongside amazing colleagues. To my PANGEA friends, thank you for welcoming me into this unique adventure.

On a personal note, I thank God for granting me strength, patience, mental clarity, and peace throughout this incredible global opportunity. I also deeply appreciate my parents for their prayers, supportive words, and inspiring foundation.

Statement of Integrity

I hereby declare that I have conducted this academic work with integrity. I confirm that I have not used plagiarism or any form of undue use of information or falsification of results during the process leading to its elaboration.

I further declare that I have fully acknowledged the Code of Ethical Conduct of the University of Minho.

A Glaciação Ordovícica Tardia no Geoparque Mundial da UNESCO Villuercas-Ibores-Jara: Sedimentologia, Petrografia e Avaliação de Geossítios.

Resumo

A sucessão do Ordovícico Superior (Hirnantiano) (Formação Gualija) localizada no sinclinal de Guadarranque no Geoparque Mundial da UNESCO Villuercas-Ibores-Jara é constituída por três membros: o Membro Risquillo, o Membro Las Majuelas e o Membro Navaldestajo. Foi efetuada uma observação, descrição e interpretação no terreno dos membros com diamictitos, seguida de uma avaliação quantitativa para determinar o seu valor científico (VS), potencial uso educativo (PEU), potencial uso turístico (PTU) e risco de degradação (DR). Os diamictitos da Formação Gualija ocorrem como uma rocha maciça não estratificada composta por uma matriz silto-argilosa escura dispersa em clastos angulares a sub-arredondados e são caracterizados por texturas mal ordenadas, suportadas pela matriz, com grãos angulares a sub-arredondados embebidos numa matriz silto-argilosa de grão fino. Este conjunto heterométrico é constituídos por partículas com tamanho que varia entre vários centrimetros e argilas.. Em lâmina delgada, os seixos alongados tendem a mostrar uma orientação preferencial, geralmente com o eixo maior paralelo à base. Como observado nas lâminas delgadas, a presença de estruturas de micro-deformação e estriamento superficial dos clastos indica uma origem glaciomarinha. As análises sedimentológicas e petrográficas revelam que estes sedimentos foram depositados por ice-rafting. A avaliação quantitativa dos geossítios quanto ao seu valor científico, turístico e educativo revela que a área de estudo possui um rico património geológico baseado na presença dos diamictitos. Estas ocorrências sãoimportantes para a investigação científica e revelam potencial geoeducativo e eventualmente geoturístico.

Palavras-chave: Diamictito, Geossítio, Formação Gualija, Petrografia, Sedimentologia.

The Late Ordovician Glaciation in the Villuercas-Ibores-Jara UNESCO Global Geopark: An Integrated Sedimentology, Petrography, and Geosite Assessment.

Abstract

The Upper Ordovician (Hirnantian) succession (Gualija Formation) located in the Guadarranque syncline within the Villuercas-Ibores-Jara UNESCO Global Geopark consists of three members: the Risquillo Member, Las Majuelas, and Navaldestajo Member. A field observation, description, and interpretations of the diamictites bearing members were done, followed by a quantitative assessment to determine the scientific value (SV), potential educational use (PEU), potential touristic use (PTU), and degradation risk (DR). The diamictites of Gualija Formation occurred as massive non-stratified rock composed of a dark silt-clay matrix spread in angular to sub-rounded clasts and are characterized by poorly sorted, matrix-supported textures with angular to sub-rounded grains embedded in a fine-grained silty-clay matrix. This heterogeneous assortment of particles ranges from clay-size grains to centimeters. In thin section, the elongated pebbles tend to show some preferred orientation, commonly with their long dimensions parallel to the bedding. As observed in the thin sections, the presence of micro-deformation structures and surficial striation of clasts indicates glaciomarine origin. Sedimentological and Petrographical analyses reveal that these sediments were deposited by ice-rafting. Quantitative assessment of geosites for scientific, touristic, and educational value reveals that the study area has rich diamictite geoheritage that holds significance for scientific research and potential for developing geo-education and possibly geotourism.

Keywords: Diamictite, Geosite, Gualija Formation, Petrography, Sedimentology.

Table of Contents

Chapter One: Introduction 1

Chapter Two: Materials and Methods 4

2.1 Geographical Location 4

2.2 Geological Setting 4

2.2.1 Structural Framework 4

2.2.2 Stratigraphy and Sedimentology 5

2.2.2.1 Ediacaran 6

2.2.2.1.1 Lower Alcudian - Domo Extremeño 6

2.2.2.1.2 Cijara Formation 6

2.2.2.2 Ediacaran-Cambrian (Terreneuvian) 6

2.2.2.2.1 Ibor Group 6

2.2.2.3 Cambrian 7

2.2.2.3.1 Pusa Formation 7

2.2.2.4 Ordovician 7

2.2.2.5 Silurian 8

2.3 Methodology 9

2.3.1 Sedimentological and Petrographical Analysis 9

2.3.2 Quantitative Assessment of Geosites 11

2.3.3 Definition of Geological Framework 16

2.3.3.1 CC-432 Navatrasierra 16

2.3.3.2 Las Majuelas 18

2.3.3.3 Garganta del Mesto 18

2.3.3.4 Arroyo Guadarranquejo 19

2.3.3.5 Charco de la Trucha 20

Chapter 3: Results 22

3.1 Sedimentology 22

3.1.1 Facies Architecture 22

3.1.2 Petrographic Observations 25

3.1.3 Facies Analysis 30

3.2 Quantitative Assessment of Geosites 31

3.2.1 Scientific Value (SV) 32

3.2.2 Degradational Risk (DR) 33

3.2.3 Potential for Educational Use (PEU) 34

3.2.4 Potential for Touristic Use (PTU) 35

Chapter 4: Discussion 36
4.1 Depositional Environment 36
4.2 Presence of Dropstones 37
4.3 Geographical extent and stratigraphic correlation 38
4.4 Geosites evaluation 39
5.0 Chapter Five: Conclusion 40
References 42
Appendix I 48

List of Figures

Figure 1. Late Ordovician paleogeographic map showing the extent of glacial cover and the location of the Iberian Peninsula (Modified from Torsvik and Cocks, 2017, fig 2.22). 2

Figure 2. The geological map and stratigraphical column of Villuercas-Ibores-Jara UNESCO Global Geopark (https://www.geoparquevilluercas.es/?lang=en) 5

Figure 3. A and B, sample collection and marking for stratigraphic orientation. (C) Sample cutting process, and (D) Samples were placed in an oven for several hours to make sure there was no moisture left 10

Figure 4. Geosite map showing locations of the five selected potential geosites indicated by stars, 1. Garganta del Mesto, 2. CC-432 Navatrasierra, 3. Las Majuelas, 4. Charco de la Trucha, 5. Arroyo Guadarranquejo............ 11

Figure 5. (A) Location of the CC-432 Navatrasierra geosite, (B) A sharp boundary between the Las Majuelas member and the Navaldestajo member at CC-432 Navatrasierra geosite, (C &D) Dropstones, CC-432 Navatrasierra geosite.. 17

Figure 6. Las Majuelas geosite. (A) General overview of Las Majuelas geosite showing all three members. (B) A scenic vista of the surrounding landscape at the Las Majuelas geosite. 18

Figure 7. (A-C) Dropstones of various sizes at the Garganta del Mesto geosite.. 19

Figure 8. (A) Location of the Arroyo Guadarranquejo geosite in the river channel during field observation. (B, C, &D) Dropstones of varying sizes from the Arroyo Guadarranquejo geosite 20

Figure 9. (A-D) Dropstones of different sizes and shapes, from angular to sub-rounded, in the Charco de la Trucha geosite. (E) An aerial view of the Transverse Fault from the Charco de la Trucha geosite. 21

Figure 10. Stratigraphic column of the measured CC-432 Navatrasierra section in the northeastern part of the Guadarranque syncline in the Villuercas-Ibores-Jara UNESCO Global Geopark. IS = Intermediate Shale, Guad. = Guadarranquejo 23

Figure 11. Photographs showing representative parts of the Risquillo and Navaldestajo members from THE Gualija Formation. (A – B) Polished slabs with a typical pattern of angular, unsorted fragments from the lower Risquillo member, from CC-432 Navatrasierra geosite. (C) Polished slab with sub-rounded, poorly sorted fragments dispersed in a coarse to fine-grained sandstone from the lower Navaldestajo member, from CC-432 Navatrasierra geosite. (D) A dropstone of probably igneous origin from the lower part of Navaldestajo, from Garganta del Mesto geosite. (E-F) Representative dropstones of angular and sub-rounded clasts from the Charco de la Trucha geosite. 24

Figure 12. A massive bed of about 10 meters with no clear stratification, from the upper part of the Risquillo member, from CC-432 Navatrasierra geosite. 25

Figure 13. (A & Ai) 40X in PPL and XPL shows pyrite, which remained dark under crossed polarization and plane polarization regardless of the stage orientation (Slide LNM5). (B & Bi) 40X in XPL and PPL shows the amorphous material observed (volcanic materials) with isotropic behaviour and remained the same in both plane-polarized and cross-polarized lights (Slide LRM6). (C & Ci) 40X in XPL and PPL shows an anisotropic mineral quartz in which optical properties are dependent on the angle and stage rotation (Slide UNM8). (D & Di) 40X in XPL and PPL shows a shale or slate fragment inclusion (Slide MNM4). All thin sections from CC-432 Navatrasierra geosite. More details in Appendix I. 28

Figure 14. (A & Ai) 40X in PPL and XPL shows monocrystalline quartz as colourless and having low relief, and in the crossed-polarized light showing higher-order colours (Slide URM5). (B & Bi) 40X in PPL and XPL shows polycrystalline or composite quartz consisting of quartz crystals in different orientations, which show different interference colours when the stage is rotated as observed in crossed polars (Slide MRM7). (C & Ci) 40X in PPL and XPL shows a sandstone fragment in which the component particles are all quartz and are easily identifiable or distinguishable even in plane-polarized light (Slide URM2). (D & Di) 40X in PPL and XPL shows shale or slate fragment inclusions that exhibit isotropism in both PPL and XPL (Slide URM4). (E & Ei) 40x in PPL and XPL shows a pyrite that remained dark under crossed polarized and plane-polarized lights, regardless of the stage orientation (Slide LRM6). (F & Fi) 40x in PPL and XPL shows a volcanic rock fragment that remained the same in both plane-

polarized and crossed polarized lights (Slide LRM3). All thin sections from CC-432 Navatrasierra geosite. More details in Appendix I 29
Figure 15.(A & Ai) 40X in XPL and PPL shows polycrystalline quartz, which shows different interference colours when the stage was rotated as observed in crossed polars and a sutured boundary between the grains (Slide LNM5). (B & Bi) 40X in XPL and PPL shows monocrystalline quartz as colourless and having low relief, and in the crossed-polarized light as white to grey (Slide LNM1). (C & Ci) 40x in XPL and PPL shows a volcanic rock fragment that remained the same in both plane-polarized and crossed-polarized lights (Slide LNM4). (D & Di) 40X in XPL and PPL shows a sandstone fragment consisting of quartz particles (Slide UNM7). (E & Ei) 40x in XPL and PPL shows a pyrite that remained dark under crossed polarized and plane-polarized lights, regardless of the stage orientation (Slide LNM5). (F & Fi) 40X in XPL and PPL shows shale or slate fragments, which are made up of fine-grained material that this magnification cannot resolve (Slide UNM1). All thin from CC-432 Navatrasierra geosite. More details in Appendix I 30
Figure 16. (A) 40x in PPL shows elongated clasts in thin sections with preferred orientation parallel to the bedding (Slide LNM4). (B) 40x in PPL shows elongated clasts in thin sections with preferred orientation parallel to the bedding (Slide UNM7). (C) 40X in PPL shows surficial striation on quartz grains (Slide LNM3). (D) 40X in PPL shows surficial striation on quartz grains (Slide LNM1). (E) 40x in PPL and XPL shows necking structures (Slide UNM8). (F) 40x in PPL and XPL shows necking structures (Slide UNM8). (G) 40x in PPL and XPL shows rotational structures (Slide MNM3). (H) 40x in PPL and XPL shows rotational structures (Slide UNM1). All thin sections are from the Navaldestajo Member, located at CC-432 Navatrasierra geosite. More details in Appendix I 31
Figure 17. Scientific values of the evaluated geosites, with CC-432 Navatrasierra having the highest value, while other geosites have moderate values. 33
Figure 18. Degradation risk assessments show Garganta del Mesto and Arroyo Guadarranquejo with moderate degradation risk, while other geosites have low degradation risk. 34
Figure 19. Potential educational use assessment of geosites showed a moderate value across all the geosites except Las Majuelas, which has a low value. 35
Figure 20. Potential touristic use for all the assessed geosites was moderate, except for Las Majuelas, which has low potential touristic value 36

List of Tables

Table 1. Criteria and respective parameters for quantitative evaluation of scientific value (SV) (Brilha 2016)... 12
Table 2. Weights of the various criteria for the final evaluation of the scientific value of geosites (Brilha 2016) 13
Table 3. Criteria and respective parameters for quantitative evaluation of degradational risk (Brilha 2016)..... 13
Table 4. Weights for the different criteria used for the assessment of degradation risk (DR) of geosites (Brilha 2016) 14
Table 5. Criteria, indicators, and parameters used for the quantitative assessment of the potential educational and touristic uses. Ten criteria (A-J) are shared between these two types of uses. Two more criteria (K-L) are used to assess PEU, and three (K-M) for PTU (Brilha 2016)........ 14
Table 6. Weights for the different criteria used for the assessment of the potential educational and touristic uses 16
Table 7. General Characterization of Thin Sections 27
Table 8. Scientific Evaluation of geosites (according to Brilha 2016)........ 32
Table 9. Degradation Risk Evaluation of geosites (according to Brilha 2016) 33
Table 10. Potential Educational Use Evaluation of geosites (according to Brilha 2016)........ 34
Table 11. Potential Touristic Use Evaluation of geosites (according to Brilha 2016) 35

Chapter One: Introduction

The Late Ordovician witnessed important geological events that involved climate change, mass extinction, and eventual biological recovery (Melchin et al. 2013; Harper et al. 2014; Jin et al. 2021). It started with the warming of the climate in the Late Katian, which was related to the changes in atmospheric carbon dioxide and temperature caused by combined processes of intense volcanism, increased continental weathering, and burial of organic carbon (Kump et al. 1999; Finlay et al. 2010; Lenton et al. 2012; Swanson-Hysell et al. 2017; Sproson et al. 2022). The cooling was initiated by the enhanced chemical weathering rate in the Late Katian that contributed to the drawdown of CO2, which corresponds to the initial cooling and further glaciation (Tang et al. 2024). Global cooling was followed in the Late Hirnantian and was characterized by weak chemical weathering intensity (Pogge Von Strandmann et al. 2017).

Several studies have been conducted to reconstruct the paleogeographic extension of the Late Ordovician glaciation (e.g, Ghienne 2003; Le Heron et al. 2004; Le Heron and Craig 2008; Torsvik and Cocks 2013, 2017; Lewin et al. 2018). Some of these studies suggest an ice sheet covering Africa, Arabia, Southern Europe, and South America (Ghienne 2003; Le Heron et al. 2004; Torsvik and Cocks, 2017), and some of these studies propose separate ice sheets with a larger one covering North Gondwana (Ghienne et al. 2007; Eyles 2008; Le Heron and Craig 2008; Torsvik and Cocks 2013; Lewin et al. 2018). The Iberian Peninsula was located at the Northern edge of Gondwana in a shallow sea oriented at approximately 60^{o}S Paleolatitude (Figure 1) (Torsvik and Cocks 2017) during the Hirnantian age, in which the icebergs floating above the shallow sea melted and deposited ice-rafted sediments. Robardet and Doré (1988) have described the geographical extent of these Hirnantian deposits in southwestern Europe and compared the results with some studies conducted in North Africa, where there is evidence of land ice (e.g, Destombes 1968, 1981; Destombes et al. 1985) and suggested that all the formations are of glacial origin.

The Late Ordovician glaciation was a short-lived glaciation event that lasted around 0.5 Ma to 1.0 Ma (Brenchley et al. 1994; Sutcliffe et al. 2000) or up to 10 Ma (Saltzman and Young 2005; Finnegan et al. 2011). Regardless of its duration, this event has left its imprint in the uppermost part of the Ordovician succession in several regions of southwestern Europe (Robardet and Doré 1988), including the Guadarranque syncline, which is part of the Villuercas-Ibores-Jara UNESCO Global Geopark in Extremadura, southern Spain.

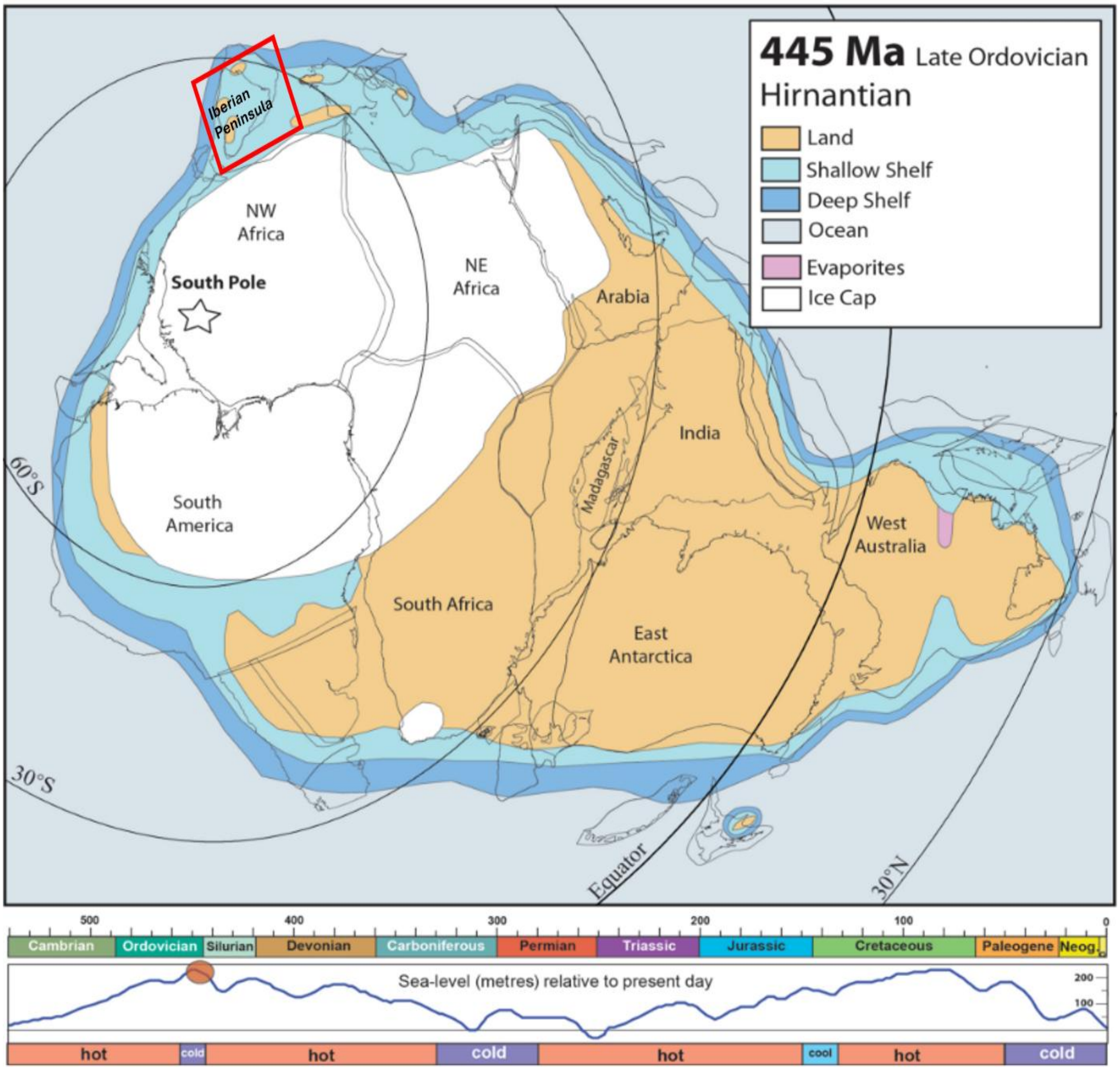

Figure 1. Late Ordovician paleogeographic map showing the extent of glacial cover and the location of the Iberian Peninsula (Modified from Torsvik and Cocks, 2017, fig 2.22).

Robardet and Doré (1988) reported that the upper part of the Ordovician succession near the Silurian boundary in many regions of southwestern Europe contains terrigenous sedimentary rocks that differ markedly from those found in the underlying Ordovician successions and the overlying Silurian layers. These sediments are composed of fine-grained argillaceous sandstones, siltstones, or silty shales containing dispersed rock fragments of varying sizes and lithologies (Robardet et al. 1988). While various interpretations have emerged regarding their origin and paleoenvironmental conditions, it is widely accepted that these sediments are linked in time to the Gondwana glaciation (Robardet and Doré 1988). These deposits have been identified in Portugal (Young 1988; Colmenar et al. 2019), the Armorican Massif, France (Doré 1981; Doré et al. 1985), Thuringia, Germany (Steiner and Falk 1981), and Spain

(Robardet et al. 1980; Robardet 1981; Fortuin 1984; Rodríguez-Núñez et al. 1989). In their earlier work, Robardet et al. (1980) were the first to distinguish these sediments from both the underlying and overlying successions in the Guadarranque syncline, describing them as "pelitas con fragmentos," meaning pelites with fragments. Rodríguez-Núñez et al. (1989) further explored the upper Ordovician Succession (Hirnantian) and reported a thickness of 20 to 80 meters and subdivided this sequence, as the Gualija Formation, into three members. Risquillo member is the lower member, and Navaldestajo is the upper member; they are made up of massive black greywackes containing clasts of heterogeneous composition and varying sizes (millimeters to decimeters), and Las Majuelas Quartzite, as the middle member, is predominantly quartzite (Rodríguez-Núñez et al. 1989).

These successions can be observed in the Guadarranque Syncline, which is a significant geological structure composed of Ordovician and Silurian sedimentary rocks, extending over a hundred kilometers in the Central Iberian Zone (Figure 2) (Rodríguez-Núñez et al. 1989). Geographically, it is located along the borders of Cáceres, Badajoz, Toledo, and Ciudad Real provinces (Rodríguez-Núñez et al. 1989). Structurally, it trends in a NW-SE direction from its northern boundary, formed by the Cenozoic materials of the Tagus Basin in the Aranuelo Field, to the Cijara Reservoir area, where it shifts to a WNW-ESE direction, changing course again at Horcajo de Los Montes (Ciudad Real), before disappearing beneath the Neogene and Quaternary materials of the La Mancha Plain near Malagon (Ciudad Real) (Rodríguez-Nuñez et al. 1989).

Previous studies on the Late Ordovician Glaciation in southwestern Europe have focused on its origin and sedimentology (e.g., Greiling 1967; Carls 1975; Fortuin 1984; and Doré et al. 1985) and its geographical extent (e.g., Robardet and Doré 1988). However, integrating these findings into geoconservation remains underdeveloped. Glaciomarine deposits in the Villuercas-Ibores-Jara UNESCO Global Geopark present an opportunity to bridge this gap by examining the Hirnantian succession (Gualija Formation) in the Guadarranque syncline and conducting a quantitative assessment of potential geosites through an accessible geosite framework, thereby promoting geoconservation, educational initiatives, public engagement, and understanding.

Therefore, this thesis aims: (1) to investigate the Late Ordovician glaciation in the Villuercas-Ibores-Jara UNESCO Global Geopark by analyzing the Gualija Formation through sedimentological and petrological interpretations, and (2) to perform a quantitative assessment of geosites for scientific value (SV) and degradational risk (DR). Furthermore, an evaluation of potential educational use (PEU) and potential touristic use (PTU) will be performed.

Chapter Two: Materials and Methods

2.1 Geographical Location

The UNESCO Global Geopark Villuercas-Ibores-Jara is situated in the southeastern part of the Spanish province of Cáceres, within the Autonomous Community of Extremadura. To the south, it borders the province of Badajoz, which is also in Extremadura, and to the east, it borders Toledo, located in the Autonomous Community of Castilla-La Mancha (Fernández Álvarez 2020). With a surface area of 2544.4 km2, the Geopark is spread across nineteen local councils with 12,883 inhabitants as of January 2019 (Fernández Álvarez 2020).

2.2 Geological Setting

2.2.1 Structural Framework

The UNESCO Global Geopark Villuercas-Ibores-Jara (Figure 2) is a mountainous region that is part of the Toledo Mountain range and lies at the heart of the Hercynian arc, connecting the Montes de Toledo with the Sierra de Monfragüe range (Fernández Álvarez 2020).

The Villuercas-Ibores-Jara UNESCO Global Geopark comprises rocks dating to approximately 580 to 400 million years. It is flanked by two Cenozoic grabens: the Tagus River to the north and the Guadiana River to the south, as well as extensive peneplains formed from Precambrian rocks to the east and west. The region features parallel mountain ridges (sierras) and valleys oriented in a northwest-southeast alignment, which emerged during the Variscan orogenic movement and were shaped by erosion in the Mesozoic era (Moreno 1974; Pulido Fernández et al. 2014).

The Cenozoic Alpine orogeny revitalized the landforms through rock fracturing and the elevation and sinking of fault blocks. Subsequently, the superimposition of the river network shaped the region's current geomorphology during the Neogene and Quaternary period (Pulido Fernández et al. 2014). This landform shares a similar origin with the North American Appalachians and is therefore commonly referred to as Appalachian relief (Pulido Fernández et al. 2014). Additionally, the relief of Las Villuercas is characterized by three modelling forms; (i) a surrounding peneplain that is made up of Ediacaran shales and greywackes, extending around the Palaeozoic synclinorium of Las Villuercas, displaying the Valdelacasa Anticline and its eroded granite batholiths to the east. (ii) The quartzite sierras serve as the primary relief element which is composed of quartzite, and they are known for their steep slopes and ridge-like crests, peaks, or crags. Their durability is due to the resistance of their rock types, namely quartzite and sandstone of the Ordovician Armorican Quartzite. (iii) The inner valleys, formed by the downcutting actions of the river network, include the valleys of the Gualija, Ibor, Viejas, Almonte, Cuernacabras, and

Garganta de Santa Lucía (which are tributaries of the River Tagus), as well as the Guadarranque, Guadalupejo, and Ruecas rivers (tributaries of the Guadiana).

2.2.2 Stratigraphy and Sedimentology

The stratigraphy of Villuercas-Ibores-Jara includes rocks of the Ediacaran, Cambrian, Ordovician, Silurian, Neogene, and Quaternary periods (Figure 2).

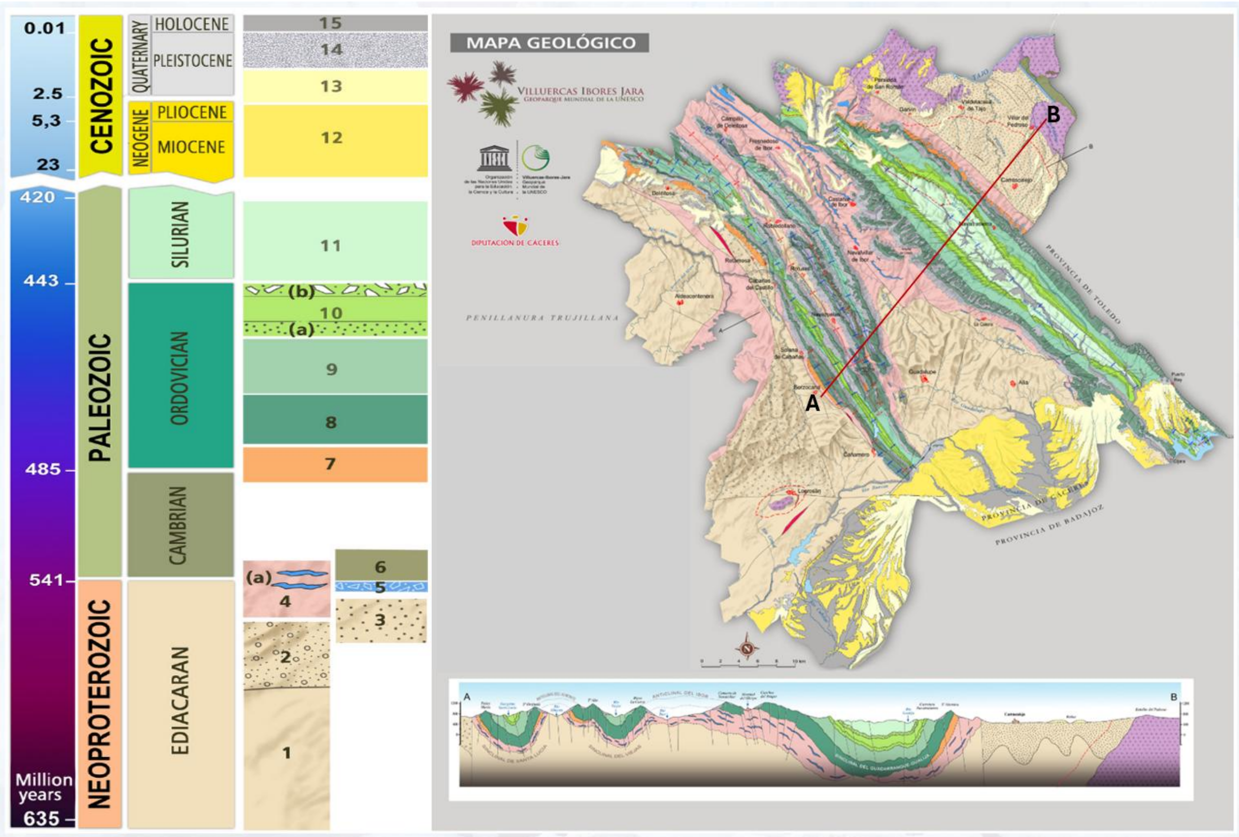

Figure 2. The geological map and stratigraphical column of Villuercas-Ibores-Jara UNESCO Global Geopark (https://www.geoparquevilluercas.es/?lang=en)

Ediacaran	Ediacaran-Cambrian (Terreneuvian)	Cambrian	Ordovician	Silurian	Cenozoic
3. Cíjara Formation	5. Olistostromes Member	6. Pusa Formation	10. Gualija Formation	11. Guadarranquejo Formation	15. Alluvium
2. Orellana Formation	4. Ibor Group		9. Intermediate Shale		14. Block Slopes and Colluvium
1. Guadiana Group			8. Armorican Quartzite		13. Raňas. Quartzite pebbles
			7. Lower Ordovician		12. Miocene red shale

2.2.2.1 Ediacaran

2.2.2.1.1 Lower Alcudian - Domo Extremeño

Recent studies (Álvaro et al. 2019) have divided the Ediacaran Lower Alcudian-Domo Extremeño into two groups: the Guadiana and Campanario groups. The Guadiana Group consists of a monotonous succession of shales and fine to coarse-grained greywackes. The Orellana Formation terminates the Campanario Group, described as "Orellana matrix-supported Conglomerates" (Pieren Pidal 2000), which reaches up to 2000 m in thickness and is composed of shales that episodically contain clast and matrix-supported rounded-to-angular clasts embedded in shales and cross-stratified conglomerates. Although far from being universally accepted, the Orellana Formation in regions close to the geopark (Orellana Dam) has recently been interpreted as of glacial origin (Linnemann et al. 2018), with alternative interpretations suggesting it is slope-related slump deposits.

2.2.2.1.2 Cijara Formation

The Orellana Formation is overlain by the Upper Ediacaran Cíjara Formation, which contains many slope-related event deposits marked by tool, bounce, and flute marks, alongside channelized deposits linked to slumps and olistostromes (Álvaro et al. 2019). The presence of limestone clasts, indicating periods of carbonate production in laterally equivalent areas, implies that the Villarta Formation of the Ibor Group (see below) was deposited concurrently with parts of the Cíjara Formation. Notably, the widespread fracturing and fissuring within a substrate subjected to episodic uplift, tilting, and block rotation is evidenced by the prevalence of hydrothermal veining and the reworking of vein quartz clast counterparts (Álvaro et al. 2019).

2.2.2.2 Ediacaran-Cambrian (Terreneuvian)

2.2.2.2.1 Ibor Group

The uppermost Ediacaran-lower Cambrian Ibor Group comprises the Castañar, Villarta, and Arrocampo formations. The Castañar Formation, reaching approximately 400 m in thickness, sits atop the Orellana Formation (Álvaro et al. 2019) and consists of shales and greywackes with minor interbedding of coarse-grained sandstone to conglomerate, along with carbonate nodules and thin layers. The Villarta Formation, which lies over the Castañar Formation (Álvaro et al. 2019), is a heterolithic sequence that varies in thickness from 100 to 250 m.

The Villarta Formation has a thickness of 100 to 250 m and can be further divided into three members in its type area on the northern shore of the Cíjara dam (Álvaro et al. 2019), from bottom to top: (i) a sequence of lenticular and bedded carbonates within greenish shales, (ii) a unit that transitions from conglomerates to sandstones and then to sandy dolostones, and (iii) a mix of shales and bedded carbonates. *Cloudina* microbial accumulations found in the lower section of the Villarta Formation (Álvaro et al. 2019) have produced specimens of *Cloudina*, *Sinotubulites*, and *Protolagena* following acid etching (Cortijo et al. 2010, 2015). *Vendotaenids* are prevalent in this member's shale interbeds, while *sabelliditids* are abundant in the second member's shale interbeds. The Arrocampo Formation (Álvaro et al. 2019) is characterized by shale dominance with increasing sandstone interbeds toward the top, featuring locally present centimetre-scale carbonate nodules aligned with stratification. This formation reaches 350 m thick and conformably overlies the Villarta Formation.

2.2.2.3 Cambrian

2.2.2.3.1 Pusa Formation

The Lower Cambrian Pusa Formation is a heterogeneous unit, reaching up to 3500 m in thickness, primarily composed of shale layers, with occasional interbeds of breccia, conglomerate, and sandstone/shale alternations, along with local carbonate interbeds and phosphorites. Álvaro et al. (2019) divided the Pusa Formation into three members. The lower member, which is approximately 1100 m thick, exhibits frequent slumping, breccia layers, and contorted beds near its base. Its basal section features clast- and matrix-supported breccias along with contorted beds rich in hydrothermal veins and clasts, transitioning upward into uniform shale interlaced with greywacke sandstone containing Cambrian-type trace fossils. Phosphatic crusts are locally prevalent.

The middle member consists of quartz-rich conglomerates that are accompanied by minor sandstones and shales that contain disseminated apatite and phosphatic crusts, characterized by finely developed lamination. The upper member has a thickness between 1900 and 2000 m and is made up of shale and greywacke sandstone, containing minor quartz-arenite interbeds and rare carbonates. This member exhibits well-developed depositional sedimentary structures and common signs of soft-sediment slumping (Álvaro et al. 2019). Compared to the underlying members of the Pusa Formation, the upper member reflects relatively shallower depositional environments (Álvaro et al. 2019).

2.2.2.4 Ordovician

Following a break in sedimentation that spanned most of the Cambrian, the Ordovician sedimentation began with a succession of shales and sandstone characterized by abundant *Skolithos*. The succeeding lower Ordovician comprises the Armorican Quartzite Formation (450-650 m) and often concludes with a variably developed sequence (20–250 m) of alternating quartzites and shales, leading into the Middle Ordovician shales (Gutiérrez-Marco et al. 2019). In some areas, this alternation is included as an upper member of the Armorican Quartzite but is frequently identified as an independent unit referred to as the Marjaliza Beds (Gutiérrez-Marco et al. 2019). Throughout most of the Iberian Massif, the remaining Ordovician strata can be categorized into two additional significant sequences. The first mainly consists of dark mudstones and siltstones, featuring varying degrees of sandstone intercalations, typically representing the Middle Ordovician. The upper sequence is less homogeneous and often incomplete in various locations, exhibiting internal unconformities. These Upper Ordovician strata are characterized by alternating layers of mudstones, siltstones, and sandstones, capped by limestone, glaciomarine diamictites, and massive quartzites (Gutiérrez-Marco et al. 2019).

Rodríguez-Nuñez et al. (1989) documented the upper Ordovician (Hirnantian) in the Guadarranque syncline, having a thickness ranging from 20m to 80m, and distinguished it into three members. The lower and upper members, the Risquillo Member and the Navaldestajo Member, respectively, are made up of massive black graywackes containing exotic pebbles of heterogeneous composition (quartzite, slate, chert, soft pebbles, volcanic rock fragments, etc.) and variable size (millimeters to decimeters). These facies have been interpreted as being of glaciomarine origin (Robardet and Doré 1988). The middle Member, or Las Majuelas Quartzite Member (Rodríguez-Nuñez et al. 1989), is predominantly made up of quartzites. The fossil content of the Gualija Formation is poor, and its age has been established using constraints from underlying and overlying fossiliferous units and lithostratigraphic criteria.

2.2.2.5 Silurian

According to (Gutiérrez-Marco et al. 2019), the onset of Silurian sedimentation was somewhat diachronic across different places in the Iberian Massif; however, the strata can be categorized into two basic successions. The first succession is prevalent across much of the Central Iberian Zone. It initiates with sandstone units at the Ordovician-Silurian transition, and euxinic black-shale sedimentation generally begins during the Late Aeronian and Telychian, continuing through the Wenlock and, in some areas, into the early Ludlow. This black shale is referred to by various names locally, including Guadarranquejo Formation in the area of Villuercas-Ibores-Jara UNESCO Global Geopark.

This black-shale succession is overlain by thick layers of alternating sandstones, siltstones, and shales from the Ludlow and Pridoli ages, which, outside of the Villuercas-Ibores-Jara UNESCO Global Geopark, are subsequently topped by sandstone and quartzite units from the earliest Devonian. Within these sand-rich sequences forming the upper part of the Silurian succession, the fossil record is limited and primarily includes shallow-water shelly faunas.

2.3 Methodology

2.3.1 Sedimentological and Petrographical Analysis

The sedimentological analysis of this study includes field observations, descriptions, and interpretations from 5 outcrops in the southwestern and northeastern parts of the Guadarranque Syncline, between the villages of Navatrasierra and Alia within the Villuercas-Ibores-Jara UNESCO Global Geopark. These exposures were measured and sampled with a focus on the Gualija Formation. Fresh samples were collected from the upper and the lower members of the Formation, at the lower, middle, and upper parts of each member (as shown in Appendix 1). Once the samples were collected, they were correctly labeled (Figure 3A and B) and marked for accurate stratigraphic orientation.

Samples collected underwent preparation at the University of Extremadura, Área de Paleontología Laboratory for microscopic (thin section) analysis. Preparation included sample cutting (Figure 3C) using a traditional rock saw to manageable sizes, allowing easier manipulation during thin section preparation. There was no need for the impregnation of the samples before cutting, as the samples are not friable and were hard enough to undergo the process without any problem. After cutting, samples were polished using a grinding station with successive grits of 120, 320, 400, and 800, and dried in an oven (Figure 3D) for several hours to make sure there was no moisture left in the samples. Petropoxy 154 epoxy resin was used to mount the samples to glass slides following the normal mounting procedures, and curing was done at a temperature between 125 – 130 degrees Celsius for about 10 minutes using a hot plate. Excess rock was trimmed using a trim saw and grinding station with successive grits of 120, 320, and 400 to grind the rock down to 100 microns. Final grinding to 30 microns was achieved using finer grits of 800, during which the thickness was monitored under a microscope using quartz birefringence. A total of 45 thin sections were made and labeled with sample names, locations, and thin-section numbers.

Petrographic analysis on each thin section was carried out using polarized light microscopy to determine grain sizes and sedimentological features on a sub-millimetre scale. These features (including lithology, grain size distribution, and sedimentary structures) allow facies association descriptions and interpretations to be made and applied to the overall diamictite-bearing succession.

Figure 3. A and B, sample collection and marking for stratigraphic orientation. (C) Sample cutting process, and (D) Samples were placed in an oven for several hours to make sure there was no moisture left

2.3.2 Quantitative Assessment of Geosites

A quantitative assessment of five geosites (Figure 4) was done using the same principles and methods described in Brilha (2016). This methodology distinguishes criteria for four distinct aspects, namely, scientific value (SV) (Table 1), potential educational use (PEU) (Table 5), potential touristic use (PTU) (Table 5), and degradation risk (DR) (Table 3). Each geosite is evaluated using a four-point scale (1-4) rating system, having indicators for each criterion. Each criterion is scored from 1 to 4 points (with zero also being a possibility). The final evaluation of scientific value, degradation risk, educational value, and touristic value of each geosite is derived from the weighted sum of these scores (Table 2; Table 4; & Table 6).

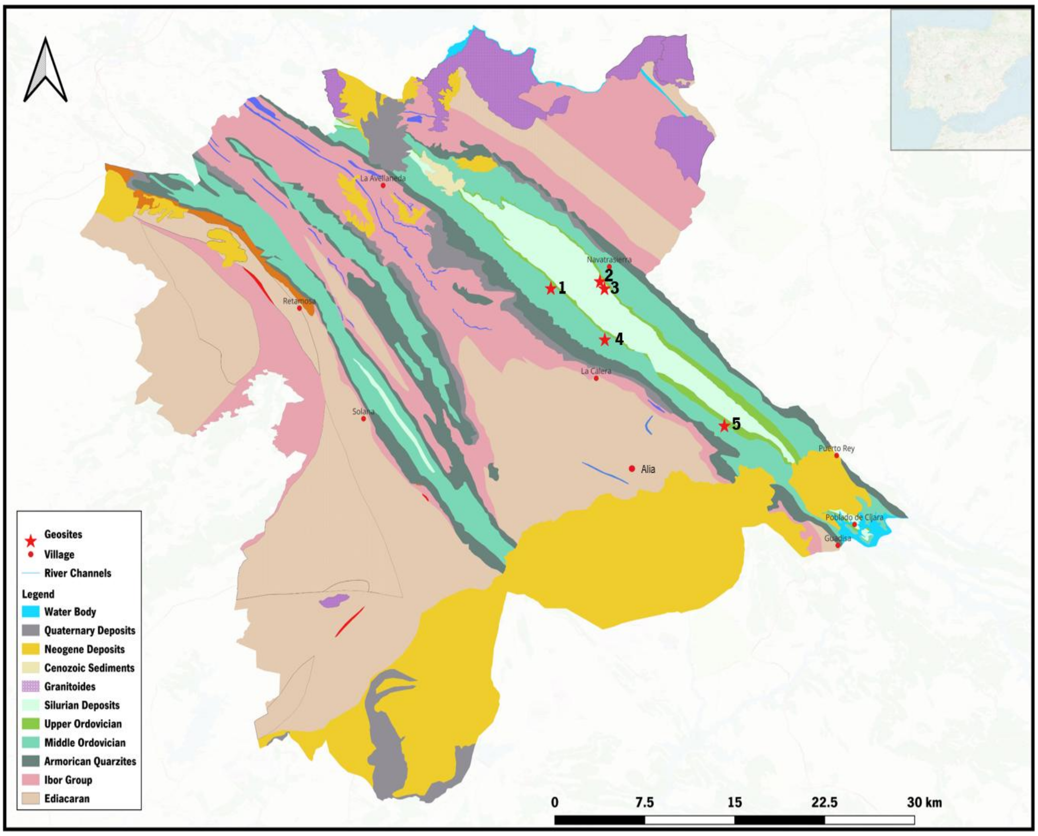

Figure 4. Geosite map showing locations of the five selected potential geosites indicated by stars, 1. Garganta del Mesto, 2. CC-432 Navatrasierra, 3. Las Majuelas, 4. Charco de la Trucha, 5. Arroyo Guadarranquejo.

Briefly, the scientific value was evaluated on seven criteria: representativeness (30%), key locality (20%), scientific knowledge (5%), integrity (15%), geological diversity (5%), rarity (15%), and use limitation (10%). Each criterion has a specific weight considering its relative importance in the evaluation of the scientific value (Tables 2.1 and 2.2). The degradation risk was assessed using the following criteria (Tables 2.3 and 2.4): deterioration of geological elements (35%), proximity to areas/activities with potential to cause degradation (20%), legal protection (20%), accessibility (15%), and density of population (10%). The degradation risk of a geosite is greatest when the geological elements have high possibility of deterioration by human and/or natural actions; it is located very close to a potentially degrading area/ activity; it does not have any legal protection nor access control; it has easy accessibility and it is located in an area with a high density of population.

Additionally, the potential educational use (Table 5) was evaluated on 12 criteria: Vulnerability (10%), Accessibility (10%), Use limitations (5%), Safety (10), Logistics (5%), Density of population (5%), Association with other values (5%), Scenery (5%), Uniqueness (5%), Observation (10%), Didactic potential (20%), and Geological diversity (10%). Furthermore, touristic potential use (Table 5) was evaluated on 13 criteria: Vulnerability (10%), Accessibility (10%), Use limitations (5%), Safety (10), Logistics (5%), Density of population (5%), Association with other values (5%), Scenery (15%), Uniqueness (10%), Observation (5%), Interpretative potential (10%), economic level (5%), and proximity of recreational areas (5%). Each criterion has a specific weight considering its relative importance in the evaluation of the potential educational and touristic uses (Tables 5 and 6).

Table 1. Criteria and respective parameters for quantitative evaluation of scientific value (SV) (Brilha 2016)

Scientific Value	
Criteria/indicators	Parameters
A. Representativeness	
The geosite is the best-known example in the geopark to illustrate elements and geological processes associated with the geological framework.	4 points
The geosite is a good example to illustrate elements and processes associated with the geological framework.	2 points
The geosite shows fairly elements and processes associated with the geological framework.	1 point
B. Key locality	
The geosite is recognised as a GSSP or ASSP by the IUGS, or is an IMA reference site	4 points
The geosite is used by the international science, directly related to the geological framework under consideration (when applicable)	2 points
The geosite is used by national science, directly related to the geological framework under consideration (when applicable)	1 point
C. Scientific knowledge	
There are scientific publications classified as A+ and A by CIRC (Clasificación Integrada de Revistas Científicas) dedicated to the geosite and associated geological framework.	4 points
There are scientific publications classified as B by CIRC (Clasificación Integrada de Revistas Científicas) dedicated to the geosite and associated geological framework	2 points
There are scientific publications classified as C by CIRC (Clasificación Integrada de Revistas Científicas) dedicated to the geosite and associated geological framework	1point
D. Integrity	
Geosite in which the main geological elements are associated with the geological framework is well preserved.	4 points
Geosite with deterioration, but that does not affect, in a decisive way, the main geological elements associated with the geological framework.	2 points
Geosite with deterioration that hinders the realisation of the main geological elements associated with the geological framework.	1 point
E. Geological Diversity	
Geosite with more than three types of different geological elements, with scientific value.	4 points
Geosite with three distinct types of geological elements, with scientific value.	2 points
Geosite with two different types of geological elements, with scientific value.	1 point

F. Rarity The geosite is the only known example in the Geopark, associated with the geological framework. There are 2 to 3 examples known in the Geopark, associated with the geological framework. There are 4 to 5 examples known in the Geopark, associated with the geological framework.	 4 points 2 points 1 points
G. Use limitation The geosite has no limitation (legal permissions, physical barriers, etc.) for sampling or fieldwork It is possible to collect samples and do fieldwork after overcoming limitations Sampling and fieldwork are very hard to carry out due to limitations difficult to overcome (legal permissions, physical barriers, etc)	 4 points 2 points 1 points

Table 2. Weights of the various criteria for the final evaluation of the scientific value of geosites (Brilha 2016)

Scientific value	
Criteria	**Weight**
A. Representativeness	30%
B. Key locality	20%
C. Scientific knowledge	5%
D. Integrity	15%
E. Geological Diversity	5%
F. Rarity	15%
G. Use limitation	10%
Total	**100%**
Total weighted	**SV**
<200 201-300 301-400	Low Moderate High

Table 3. Criteria and respective parameters for quantitative evaluation of degradational risk (Brilha 2016)

Degradation risk	**Parameter**
A. Deterioration of contents	
Possibility of deterioration of all geological elements	4 points
Decaying possibility of major geological elements	2 points
No possibility of deterioration of the main geological elements 1 point.	1 point
B. Proximity to potentially degrading areas	
Geosite situated less than 50 m from a potentially degrading activity	4 points
Geosite situated less than 250 m from a potentially degrading activity	2 points
Geosite situated less than 500 m from a potentially degrading activity.	1 point
C. Protection regime	
Geosite is located in an area with no system of legal protection and without access control	4 points
Geosite is located in an area with no system of legal protection and access control	2 points
Geosite is located in an area with legal protection arrangements and access control	1 point
D. Accessibility	
Geosite situated less than 100 m from a road	4 points
Geosite situated between 100 and 500 m from the road	2 points
Geosite situated more than 500 m from a road	1 point
E. Density	
Geosite in municipalities with over 1000 inhabitants/km2	4 points
Geosite in municipalities with over 166 and less than 1000 inhabitants/km2	2 points
Geosite in town with less than 166 inhabitants/km2	1 point

Table 4. Weights for the different criteria used for the assessment of degradation risk (DR) of geosites (Brilha 2016)

Degradation risk		
Criteria		**Weight**
A. Deterioration of geological elements		35%
B. Proximity to areas/activities with potential to cause degradation		20%
C. Legal protection		20%
D. Accessibility		15%
E. Density of population		10%
Total		**100%**
Total weighted	**Degradation risk**	
<200	Low	
201-300	Moderate	
301-400	High	

Table 5. Criteria, indicators, and parameters used for the quantitative assessment of the potential educational and touristic uses. Ten criteria (A-J) are shared between these two types of uses. Two more criteria (K-L) are used to assess PEU, and three (K-M) for PTU (Brilha 2016).

Potential Educational and Touristic Use	
Criteria/indicators	Parameters
A. Vulnerability	
The geological elements of the geosite present no possible deterioration from anthropogenic activity	4 points
There is the possibility of deterioration of secondary geological elements by anthropogenic activity	3 points
There is the possibility of deterioration of the main geological elements by anthropogenic activity	2 points
There is the possibility of deterioration of all geological elements by anthropogenic activity	1 point
B. Accessibility	
The site is located less than 100 m from a paved road and with bus parking.	4 points
Site located less than 500 m from a paved road	3 points
Site accessible by bus, but through a gravel road	2 points
Site with no direct access by road, but located less than 1 km from a road accessible by bus	1 point
C. Use limitations	
The site has no limitations to be use by students and tourists	4 points
The site can be used by students and tourists, but only occasionally	3 points
The site can be used by students and tourists, but only after overcoming limitations (legal, permissions, physical, tides, floods, ...)	2 points
The use by students and tourists is very hard to accomplish due to limitations difficult to overcome (legal, permissions, physical, tides, floods...)	1 point
D. Safety	
Site with safety facilities (fences, stairs, handrails, etc.), mobile phone coverage, and located less than 5 km from emergency services	4 points
Site with safety facilities (fences, stairs, handrails, etc.), mobile phone coverage, and located less than 25 km from emergency services	3 points
Site with no safety facilities but with mobile phone coverage and located less than 50 km from emergency services	2 points
Site with no safety facilities, no mobile phone coverage, and located more than 50km from emergency services	1 point
E. Logistics	
Lodging and restaurants for groups of 50 persons, less than 15 km away from the site	4 points
Lodging and restaurants for groups of 50 persons, less than 50 km away from the site	3 points
Lodging and restaurants for groups of 50 persons, less than 100 km away from the site	2 points
Lodging and restaurants for groups of less than 25 persons and less than 50 km away from the site	1 point

F. Density of population	
The site is located in a municipality with more than 1000 inhabitants/Km^2	4 points
Site located in a municipality with 250-1000 inhabitants/km^2	3 points
Site located in a municipality with 100-250 inhabitants/km^2	2 points
Site located in a municipality with fewer than 100 inhabitants/km^2	1 point
G. Association with other values	
The occurrence of several ecological and cultural values is less than 5 km away from the site	4 points
The occurrence of several ecological and cultural values is less than 10 km away from the site	3 points
The occurrence of one ecological value and one cultural value less than 10 km away from the site	2 points
The occurrence of one ecological or cultural value less than 10 km away from the site	1 point
H. Scenery	
The Site currently used as a tourism destination in national campaigns	4 points
The Site is occasionally used as a tourism destination in national campaigns	3 points
The Site is currently used as a tourism destination in local campaigns	2 points
The site is occasionally used as a tourism destination in local campaigns	1 point
I. Uniqueness	
The site shows unique and uncommon features, considering this and neighbouring countries	4 points
The site shows unique and uncommon features in the country	3 points
The site shows common features in this region, but they are uncommon in other regions of the country	2 points
The site shows features rather common in the whole country	1 point
J. Observation conditions	
All geological elements are observed in good condition	4 points
There are some obstacles that make difficult the observation of some geological elements	3 points
There are some obstacles that make difficult the observation of the main geological elements	2 points
There are some obstacles that almost obstruct the observation of the main geological elements	1 point

Potential Educational Use		**Potential Touristic Use**	
K. Didactic potential		K. Interpretative potential	
The site presents geological elements that are taught at all teaching levels	4 points	The site presents geological elements in a very clear and expressive way to all types of public	4 points
The site presents geological elements that are taught in elementary schools	3 points	The public needs to have some geological background to understand the geological elements of the site	3 points
The site presents geological elements that are taught in secondary schools	2 points	The public needs to have a solid geological background to understand the geological elements of the site	2 points
The site presents geological elements that are taught at the university	1 point	The site presents geological elements only understandable to geological experts.	1 point
L. Geological diversity		L. Economic level	
More than 3 types of geodiversity elements occur in the site (mineralogical, palaeontological, geomorphological, etc)	4 points	The site is located in a municipality with a household income at least double the national average	4 points
There are 3 types of geodiversity elements in the site	3 points	The site is located in a municipality with a household income higher than the national average	3 points
There are 2 types of geodiversity elements in the site	2 points	The site is located in a municipality with a household income similar to the national average	2 points
There is only 1 type of geodiversity element in the site	1 point	The site is located in a municipality with a household income lower than the national average	1 point
		M. Proximity of recreational areas	

		Site located less than 5 km from a recreational area or tourist attraction	4 points
		Site located less than 10 km from a recreational area or tourist attraction	3 points
		Site located less than 15 km from a recreational area or tourist attraction	2 points
		Site located less than 20 km from a recreational area or tourist attraction	1 point

Table 6. Weights for the different criteria used for the assessment of the potential educational and touristic uses

Potential use			
Educational	Weight	Touristic	Weight
A. Vulnerability	10%	A. Vulnerability	10%
B. Accessibility	10%	B. Accessibility	10%
C. Use limitations	5%	C. Use limitations	5%
D. Safety	10%	D. Safety	10%
E. Logistics	5%	E. Logistics	5%
F. Density of population	5%	F. Density of population	5%
G. Association with other values	5%	G. Association with other values	5%
H. Scenery	5%	H. Scenery	15%
I. Uniqueness	5%	I. Uniqueness	10%
J. Observation	10%	J. Observation	5%
K. Didactic potential	20%	K. Didactic potential	10%
L. Geological diversity	10%	L. Economic level	5%
		M. Proximity of recreational areas	5%
Total	**100%**	**Total**	**100%**
Total weighted		**EPU/PTU**	
<200		Low	
201-300		Moderate	
301-400		High	

2.3.3 Definition of Geological Framework

The geosite inventory method's definition relies on the inventory's aim, addressing four points: object, value, scope, and utility (Lima et al. 2010). For this study, it was decided to identify and select only geosites related to the Late Ordovician glaciation within the Villuercas-Ibores-Jara UNESCO Global Geopark. An integrated literature review and field observations of each geosite among the 5 selected geosites in the geopark (Figure 4) were done. Field studies were conducted to provide descriptions of rock outcrops and the current state of each geosite, as well as to document them, while the literature review (e.g., Rodriguez-Núñez et al. 1989) was undertaken to enrich field descriptions and to interpret the geological processes associated with the geosites. The employed methodology includes inventory and quantitative assessment of geosites related to the Hirnantian glaciation in the Villuercas-Ibores-Jara UNESCO Global Geopark.

2.3.3.1 CC-432 Navatrasierra

The CC-432 Navatrasierra is located at 39,59896° N, -5,25039° W alongside CC-432 road, approximately 1 kilometre from Navatrasierra. It is easily accessible via the CC-432 road (Figure 5A). This site represents the best example in the study area concerning the geological framework under study. The entire Gualija Formation is exposed here, and the boundaries (Figure 5B, boundary between Las Majuelas and the Navallestajo members) between all three members of the formation are visible. Additionally, the underlying Middle Ordovician succession and the overlying Silurian succession can be observed at this geosite. There are several articles published in international and national journals directly related to the geosite (e.g., Fortuin 1984; Doré et al. 1985; Robardet and Doré 1988; Rodríguez-Núñez et al. 1989) because the Late Ordovician glaciation has been a topic of discussion and debate for over five decades in southwestern Europe. Dropstones (Figure 5C & D) of various sizes (ranging from 1cm to 5cm) can be observed. The geological diversity includes dropstones, stratigraphy, and the fossil content of the overlying black shale. Furthermore, there are no use limitations related to this geosite, and accessibility is very easy due to its location by the roadside.

Figure 5. (A) Location of the CC-432 Navatrasierra geosite, (B) A sharp boundary between the Las Majuelas member and the Navaldestajo member at CC-432 Navatrasierra geosite, (C &D) Dropstones, CC-432 Navatrasierra geosite.

2.3.3.2 Las Majuelas

Las Majuelas (Figure 6A) is located at 39,59293°N, -5,246000°W. It is the type locality for the Majuelas Member. The site can be accessed from Navatrasierra village via CC432 road, about 1.8 kilometers west of Navatrasierra, and on an unpaved road, approximately 1 kilometer from CC-432 road that requires a 4x4 vehicle or hiking due to rough terrain. The geosite has a scenic vista due to its surrounding landscape (Figure 6B), but it is not currently being used as a tourist destination or for promoting geotourism. Additionally, it is located in a remote area, a little far from the road, and it is difficult to access due to rugged terrain.

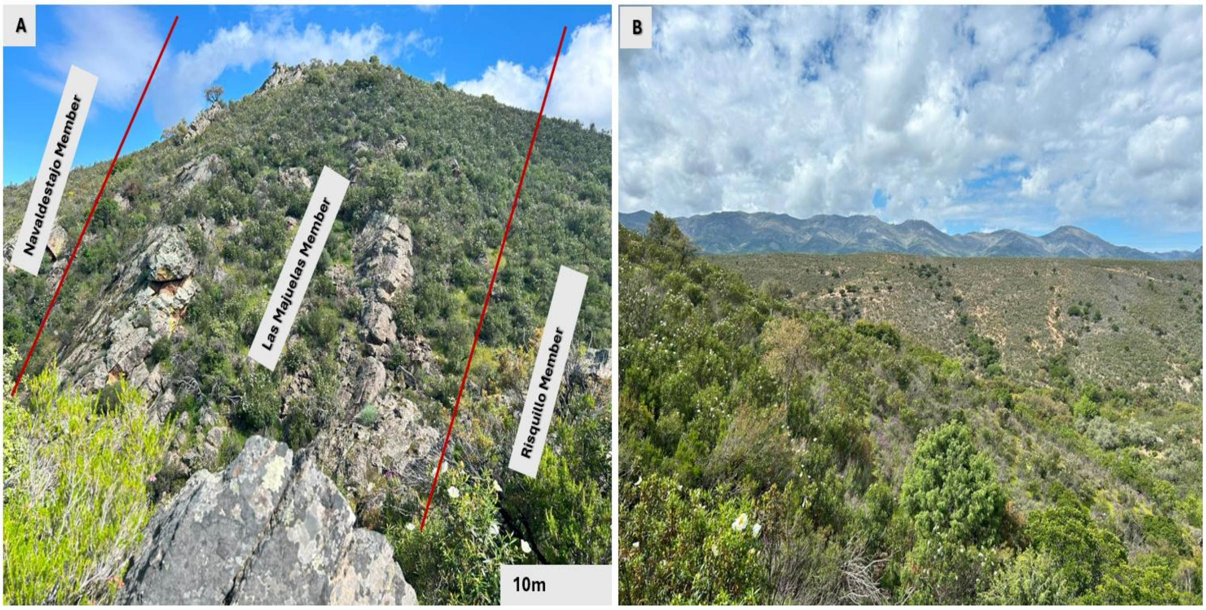

Figure 6. Las Majuelas geosite. (A) General overview of Las Majuelas geosite showing all three members. (B) A scenic vista of the surrounding landscape at the Las Majuelas geosite.

2.3.3.3 Garganta del Mesto

This geosite is located in a river channel at 39,59314°N -5,29778°W, about 5 kilometers as the crow flies from Navatrasierra and can be reached via CC-432 road with a distance of approximately 9 km west of Navatrasierra. The geosite is about 300 meters away from the road, and the difficulty in accessing this site is between easy to moderate, depending on the fitness level of the visitor and familiarity with outdoor terrain. The main geological elements under study are in good observational conditions, as shown in Figure 7A-C.

Figure 7. (A-C) Dropstones of various sizes at the Garganta del Mesto geosite.

2.3.3.4 Arroyo Guadarranquejo

This geosite is located at N39,47810° N, -5,13039° W in the Arroyo Guadarranquejo channel, about 11 kilometers by road from the village of Alia and about 8.30 kilometers as the crow flies from the same village. Arroyo Guadarranquejo (Figure 8A) is easily accessible via the EX-102 road from the village of Alia. The main geological elements, diamictites and Silurian graptolite-rich shale, can be observed in good condition (Figure 8B-D), and the site has no use limitation apart from the low fence that can easily be skipped over.

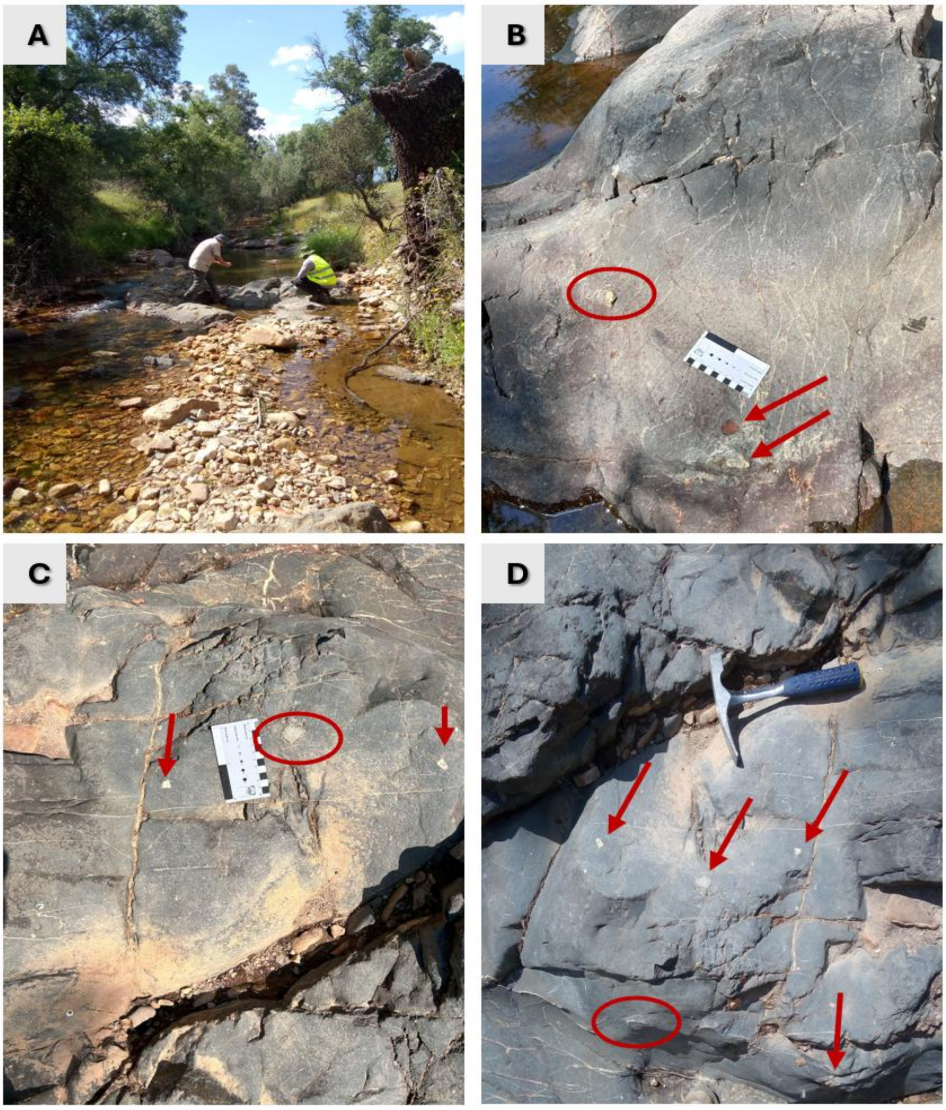

Figure 8. (A) Location of the Arroyo Guadarranquejo geosite in the river channel during field observation. (B, C, &D) Dropstones of varying sizes from the Arroyo Guadarranquejo geosite

2.3.3.5 Charco de la Trucha

This geosite is located in a river channel at 39,55018°N -5,24575°W, about 11.5 kilometres from Navatrasierra via CC-432 road (about 5km from Navatrasierra) and unpaved road (about 6.5km from CC-432 road) that requires a 4x4 vehicle. Charco de la Trucha is located in a river channel, and just ahead of the diamictites-bearing formation (Figure 9A-D) lies the quartzites with amazing, stepped waterfalls. The geosite is also located close to a small transverse fault (Figure 9E) that has fractured quartzites. It currently figures as a geosite within the Villuercas-Ibores-Jara Geopark (https://geoparquevilluercas.es/no28-cancheras-de-la-trucha/).

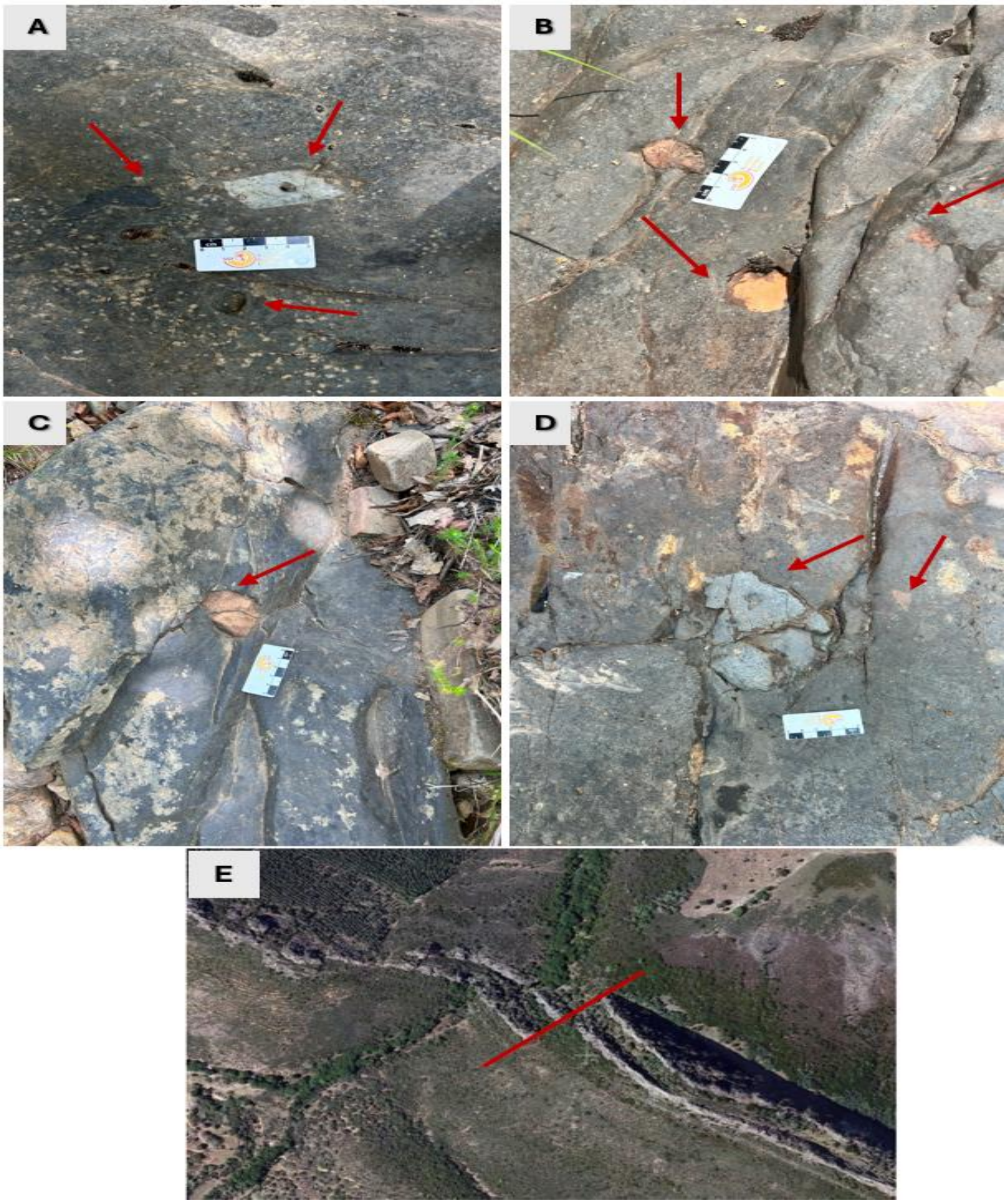

Figure 9. (A-D) Dropstones of different sizes and shapes, from angular to sub-rounded, in the Charco de la Trucha geosite. (E) An aerial view of the Transverse Fault from the Charco de la Trucha geosite.

Chapter 3: Results

3.1 Sedimentology

The underlying focus of this study reflects the sedimentological observations based on a macroscopic and microscopic approach of five localities along the Guadarranque syncline in the Villuercas-Ibores-Jara UNESCO Global Geopark between the villages of Navatrasierra and Alia. Presented herein are observations, descriptions, and interpretations of diamictites bearing members of the Gualija Formation. It is important, however, to note that only the CC-432 Navatrasierra outcrop/geosite has been logged because of its completeness and general exposure. The rest of the outcrops are not completely exposed, but significant portions of them are exposed. Moreover, sites like Charco de la Trucha, Garganta del Mesto, and Arroyo Guadarranquejo are variably exposed seasonally due to their locations in river channels.

3.1.1 Facies Architecture

In the Guadarranque syncline within the Villuercas-Ibores-Jara UNESCO Global Geopark, five outcrops (potential geosites) between Navatrasierra and Alia prominently display the Gualija Formation. This Formation is divided into three members exhibiting stratigraphic disparity and reaches a thickness of up to 144 meters (Fig. 10). The Risquillo and Navaldestajo members contain heterometric clasts with particle sizes ranging from less than millimeters to centimeters (Figure 11A-F), and are dark gray to black, and sometimes medium gray (when weathered). These clasts are poorly sorted and vary from angular to subrounded (Figure 11A-C), in which the oblong clasts tend to be oriented parallel to the bedding as observed in the thin section. These facies are unstratified and often lack clear bedding planes over significant thicknesses (5–10 m) (Figure 12), although fractures can sometimes resemble bedding planes.

The logged section (CC-432 Navatrasierra) is located along CC-432 road (Figure 10) in the northeastern part of the syncline, near the village of Navatrasierra. The entire Gualija Formation, comprising all three members, is visible and well-exposed along the road cut, revealing its upper and lower boundaries. The lower member (Risquillo Member) measures 54 m. While the boundary between the Risquillo Member and the underlying middle Ordovician shale (Intermediate Shale) is not well exposed, approximately 2 meters of sandstone quartzite separates them. The middle member (Las Majuelas) is measured at 40 m and is predominantly quartz sandstone. The boundary between the lower member and the middle member is sharp, likely due to scouring of the overlying sandstone. The upper member (Navaldestajo Member) measures 50 m and has a sharp boundary with the middle member (Las Majuelas). About 1.5

meters of quartzite lies above the Navaldestajo member before it transitions to the overlying Silurian black shale.

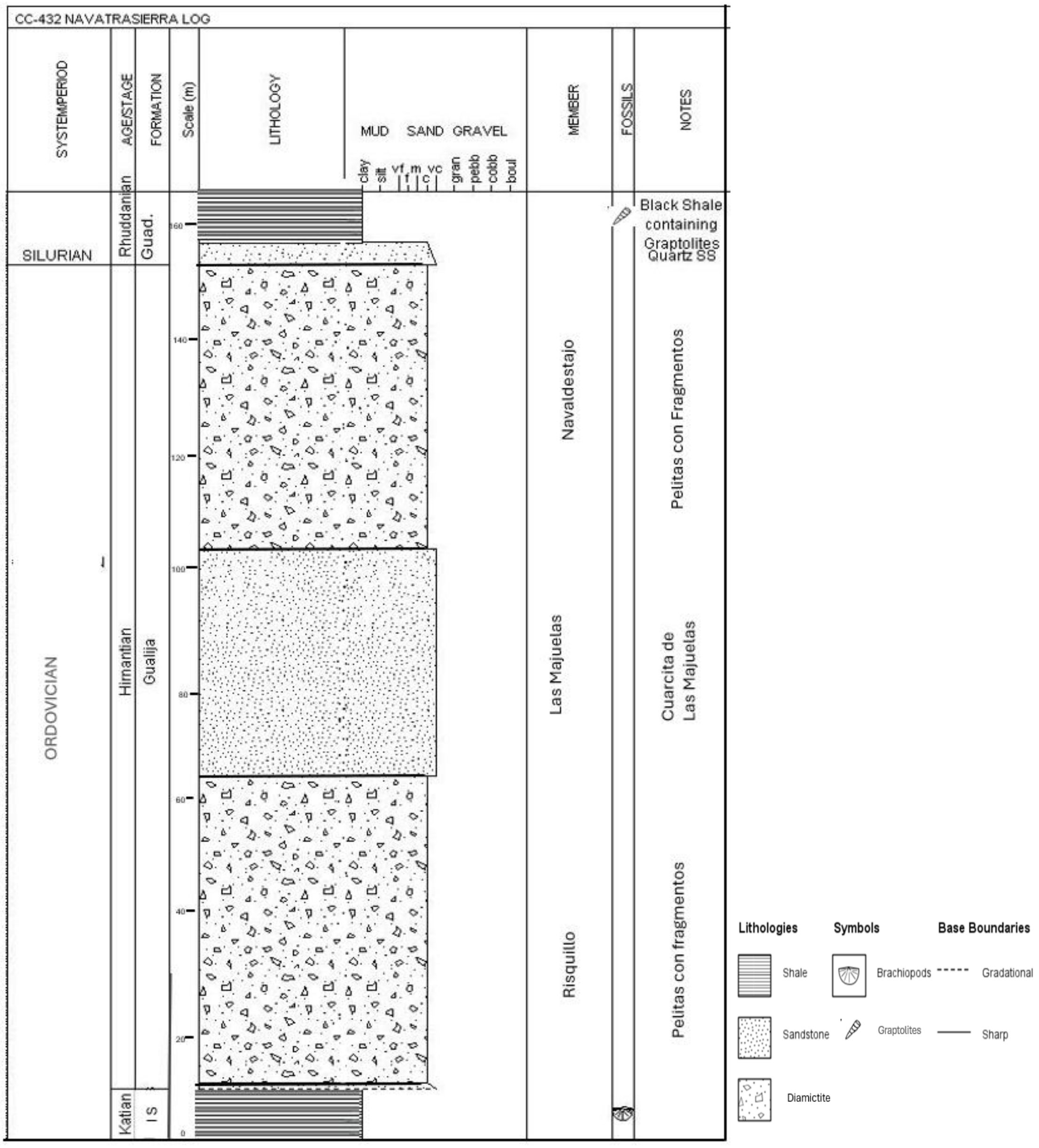

Figure 10. Stratigraphic column of the measured CC-432 Navatrasierra section in the northeastern part of the Guadarranque syncline in the Villuercas-Ibores-Jara UNESCO Global Geopark. IS = Intermediate Shale, Guad. = Guadarranquejo

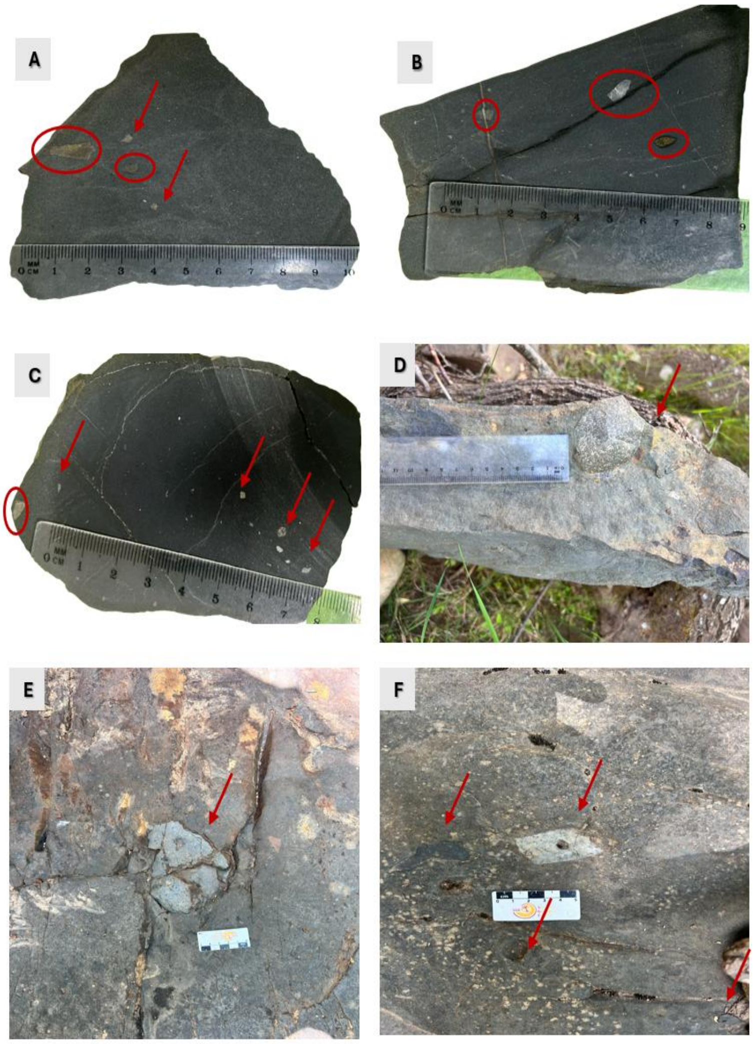

Figure 11. Photographs showing representative parts of the Risquillo and Navaldestajo members from THE Gualija Formation. (A – B) Polished slabs with a typical pattern of angular, unsorted fragments from the lower Risquillo member, from CC-432 Navatrasierra geosite. (C) Polished slab with sub-rounded, poorly sorted fragments dispersed in a coarse to fine-grained sandstone from the lower Navaldestajo member, from CC-432 Navatrasierra geosite. (D) A dropstone of probably igneous origin from the lower part of Navaldestajo, from Garganta del Mesto geosite. (E-F) Representative dropstones of angular and sub-rounded clasts from the Charco de la Trucha geosite.

Figure 12. A massive bed of about 10 meters with no clear stratification, from the upper part of the Risquillo member, from CC-432 Navatrasierra geosite.

3.1.2 Petrographic Observations

The general petrographic observation made includes isotropic minerals, Anisotropic minerals, and amorphous materials. The isotropic mineral (pyrite) (Figure 13A & Ai) shows the same optical properties in all directions and does not split light into two rays (no birefringence) and remains dark under crossed polarization and plane polarization regardless of the stage orientation. It appears opaque, completely black, regardless of stage rotation; no pleochroism was observed in transmitted light or reflected light, and the shape observed in all the thin sections was cubic. Anisotropic mineral (e.g, quartz) (Figure 13C & Ci) has direction-dependent optical properties as observed in the microscope. They showed birefringence and varying colours under crossed polarization as the microscope stage is rotated. In crossed polars, interference colours vary with orientation, with extinction at every 90 degrees. The amorphous material observed (volcanic materials) (Figure 13B & Bi) lacked a long-range crystal structure as they are not truly crystalline and did not show any ordered atomic arrangement needed for standard optical properties. No colour changes between plane-polarized and crossed-polarized lights, and there was no pleochroism or extinction when the stage was rotated; it was generally dull. The behaviour was isotropic and remained the same in both plane-polarized and cross-polarized lights. Shale fragments (Figure 13D & Di) appeared dark in both plane-polarized and cross-polarized lights.

Based on Folk's (1951) scale of textural maturity classification, the general textural maturity of sediments in the study area ranges between the immature stage and sub-mature stage, as observed in the thin section, as the grains are poorly sorted and contain grains that are angular to sub-rounded. Thin-section analysis in both Risquillo and Navaldestajo members shows a poorly sorted silty, micaceous/clay matrix featuring a variety of quartz grains (monocrystalline and polycrystalline quartz), volcanic rock fragments, shale/slate fragments, sedimentary rock fragments, and pyrite that range from sub-rounded to angular, as well as mica (more muscovite) and some rare plagioclase. The dark, fine-grained cement comprises a clay/micaceous matrix surrounding the larger grains.

The lower part of the Risquillo Member shows a poorly sorted texture in a fine-grained matrix. It is composed of polycrystalline and monocrystalline quartz. The monocrystalline quartz is easily identifiable in plane polarized light by its colourlessness and having low relief and in the crossed-polarized light as white to grey. The polycrystalline or composite quartz consists of quartz crystals in different orientations, which show different interference colours when the stage is rotated as observed in crossed polars. Additionally, the boundary between the grains is sutured, which suggests a metamorphic origin. There is also pyrite, volcanic rock fragments, and sedimentary rock fragments dispersed in a fine-grained matrix. The middle part of the Risquillo Member is also predominantly quartz, with a sandstone fragment in which the component particles are all quartz and are easily identifiable or distinguishable even in plane-polarized light. The Upper part of the Risquillo Member contains shale/slate fragments that are made up of fine-grained material, which cannot be resolved at this magnification. They have a characteristic of platy shape as a result of derivation from a cleaved source rock containing abundant platy minerals. Additionally, this part also contains volcanic rock fragments, both monocrystalline and polycrystalline quartz, sedimentary rock fragments, and pyrite. Generally, the Risquillo Member comprises of quartz (monocrystalline and polycrystalline) (Figure 14A & Bi, b & Bi), volcanic rock fragments (Figure 14F & Fi), pyrite (Figure 14E & Ei), sedimentary rock fragments (Figure 14C & Ci), and shale fragments (Figure 14D & Di) with varying sizes ranging from very angular grain to sub-round grains. Important microstructures observed include fractures, rotational structures, necking structures, and surficial striation marks.

The lower Navaldestajo Member contains quartz fragments (monocrystalline quartz and polycrystalline), volcanic rock fragments, sedimentary rock fragments, and pyrites in minute quantities. The middle part of the Navaldestajo Member contains predominantly quartz (monocrystalline quartz and polycrystalline), sedimentary rock fragments, and shale/slate fragments. The upper part of the Navaldestajo Member contains shale/slate fragments, a few volcanic rock fragments, quartz, and sedimentary rock fragments. There are also microstructures observed, such as rotational structures, necking structures, fractures, and surficial striations. In general, Navaldestajo Member comprises of quartz (monocrystalline and polycrystalline) (Figure 15 A & Ai, B & Bi), volcanic rock fragments (Figure 15C & Ci), pyrite (Figure 15E & Ei), sedimentary rock fragments (Figure 15D & Di), and shale fragments (Figure 15F & Fi) with varying sizes ranging from very angular grain to sub-round grains.

Both Risquillo and Navaldestajo members consist of the fragments of quartz, shale/slate fragments, volcanic rock fragments, sedimentary rock fragments, and pyrite. The coarse clastic materials observed include unsorted grains, varying from millimetric grains to decimetric grains, with shapes ranging from angular to sub-rounded. These clasts are unevenly distributed: larger stones are often isolated, with certain horizons exhibiting a greater concentration of clasts, while others display only coarse millimetric quartz grains. Large fragments are clasts of sedimentary rocks, volcanic rocks, and quartz.

Table 7. General Characterization of Thin Sections

General Characterization of Thin Sections	
1. Textural Analysis	
A. Skeleton	
• Size ranges	Clay/silt/sand (<0.5 - >1mm)
• Particle shape and form	Angular to sub-rounded
• Composition	Dominantly quartz, pyrite, volcanic rocks, sedimentary rocks, and shale/slate fragments.
B. Matrix	
• Texture	
• Distribution	Clay/silty matrix
2. Structural Analysis	
A. Structures	
• Sedimentary structures	—
• Deformation structures	Necking structures, rotational structures, and dropstones.
• Diagnostic features of a specific environment	
• Diagenesis and post-depositional alteration	—
3. Interpretation	Ice-rafted debris in proximal glaciomarine settings

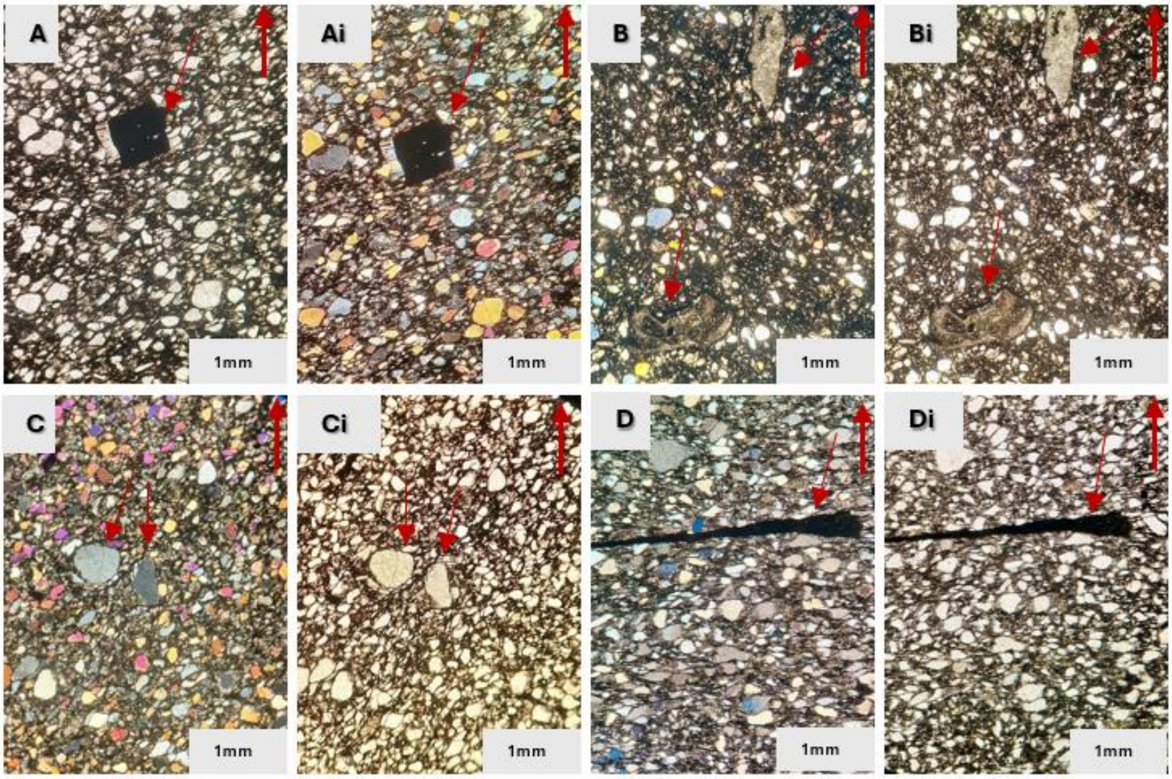

Figure 13. (A & Ai) 40X in PPL and XPL shows pyrite, which remained dark under crossed polarization and plane polarization regardless of the stage orientation (Slide LNM5). (B & Bi) 40X in XPL and PPL shows the amorphous material observed (volcanic materials) with isotropic behaviour and remained the same in both plane-polarized and cross-polarized lights (Slide LRM6). (C & Ci) 40X in XPL and PPL shows an anisotropic mineral quartz in which optical properties are dependent on the angle and stage rotation (Slide UNM8). (D & Di) 40X in XPL and PPL shows a shale or slate fragment inclusion (Slide MNM4). All thin sections from CC-432 Navatrasierra geosite. More details in Appendix I.

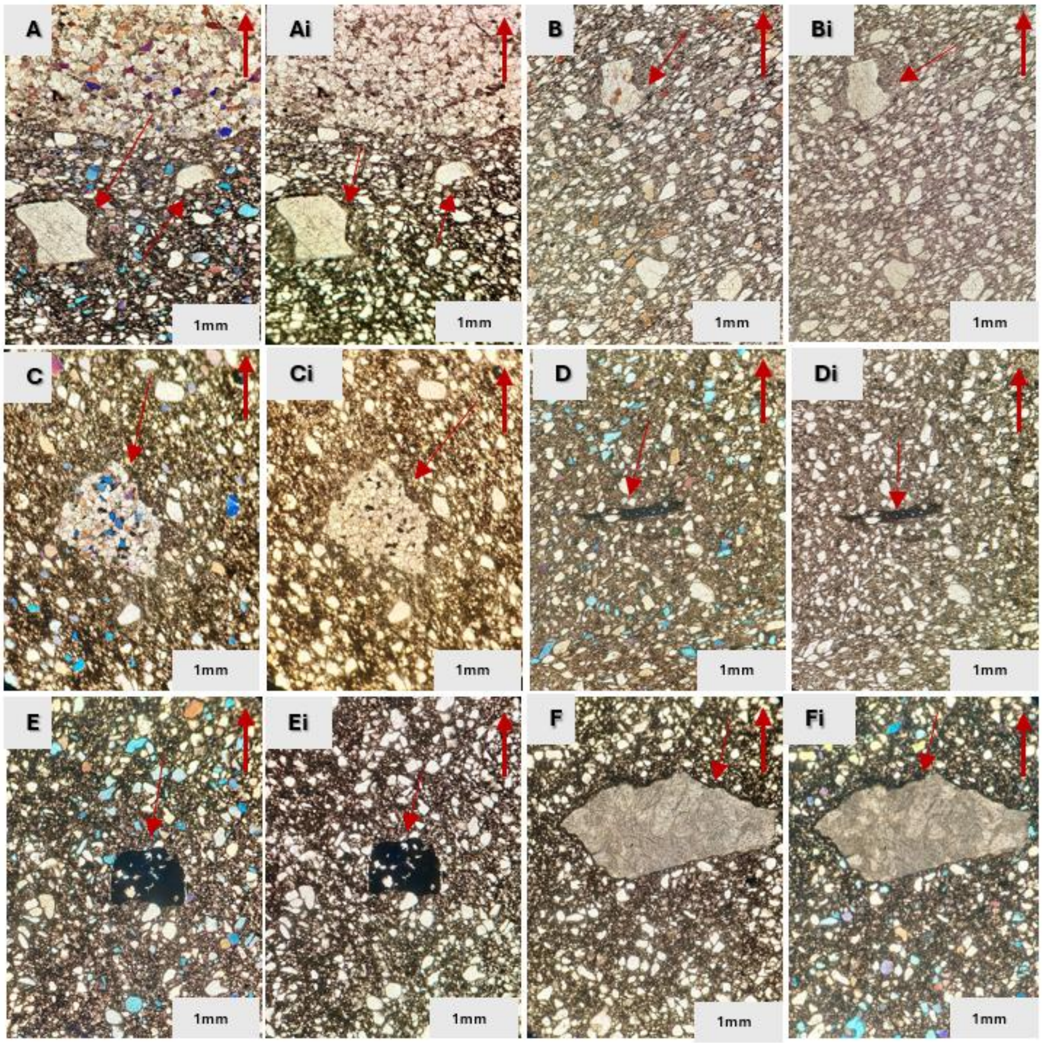

Figure 14. (A & Ai) 40X in PPL and XPL shows monocrystalline quartz as colourless and having low relief, and in the crossed-polarized light showing higher-order colours (Slide URM5). (B & Bi) 40X in PPL and XPL shows polycrystalline or composite quartz consisting of quartz crystals in different orientations, which show different interference colours when the stage is rotated as observed in crossed polars (Slide MRM7). (C & Ci) 40X in PPL and XPL shows a sandstone fragment in which the component particles are all quartz and are easily identifiable or distinguishable even in plane-polarized light (Slide URM2). (D & Di) 40X in PPL and XPL shows shale or slate fragment inclusions that exhibit isotropism in both PPL and XPL (Slide URM4). (E & Ei) 40x in PPL and XPL shows a pyrite that remained dark under crossed polarized and plane-polarized lights, regardless of the stage orientation (Slide LRM6). (F & Fi) 40x in PPL and XPL shows a volcanic rock fragment that remained the same in both plane-polarized and crossed polarized lights (Slide LRM3). All thin sections from CC-432 Navatrasierra geosite. More details in Appendix I

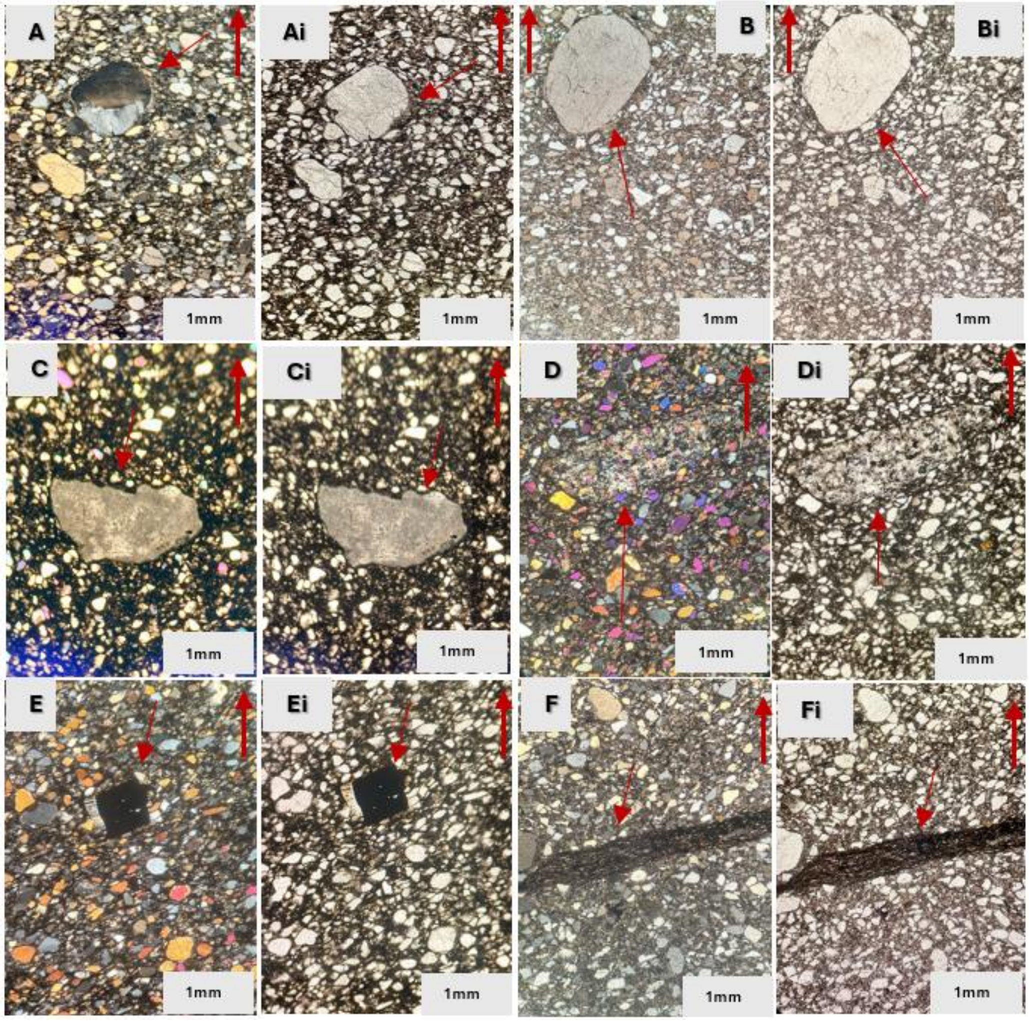

Figure 15.(A & Ai) 40X in XPL and PPL shows polycrystalline quartz, which shows different interference colours when the stage was rotated as observed in crossed polars and a sutured boundary between the grains (Slide LNM5). (B & Bi) 40X in XPL and PPL shows monocrystalline quartz as colourless and having low relief, and in the crossed-polarized light as white to grey (Slide LNM1). (C & Ci) 40x in XPL and PPL shows a volcanic rock fragment that remained the same in both plane-polarized and crossed-polarized lights (Slide LNM4). (D & Di) 40X in XPL and PPL shows a sandstone fragment consisting of quartz particles (Slide UNM7). (E & Ei) 40x in XPL and PPL shows a pyrite that remained dark under crossed polarized and plane-polarized lights, regardless of the stage orientation (Slide LNM5). (F & Fi) 40X in XPL and PPL shows shale or slate fragments, which are made up of fine-grained material that this magnification cannot resolve (Slide UNM1). All thin from CC-432 Navatrasierra geosite. More details in Appendix I

3.1.3 Facies Analysis

Both the Risquillo Member and the Navaldestajo Member consist of poorly sorted, silty/clay matrix diamictites with no overall preferred orientation of the grains, as they are rather oriented in a random manner throughout. However, the elongated clasts in thin sections (Figure 16A & B) tend to show preferred orientation, commonly with their long dimensions parallel to the bedding. Additionally, grain surface textures are generally rough, with fractures in some cases, and surficial striations (Figure 16C & D). These chaotic fragment distributions contain angular to subrounded clasts of less than 1mm as observed in thin sections embedded in a fine-grained silty-clay matrix, to a few centimetres as observed in the field. The composition of these diamictite-bearing members is likely to be derived from the basement rocks, volcanic rocks, and recycled older sedimentary rocks. Microstructures include necking (Figure 16E & F), rotational structures (Figure 16G & H), and surficial striations on quartz grains (Figure

16C & D). A general dispersion of dropstones (less than 1mm to 5cm) exists throughout. These dropstones have formed necking structures indicating deposition from rafted ice (Boggs, 1995). There is a complete absence of both trace and body fossils in the Gualija Formation, as acritarch analysis yielded a negative result (Teodoro Palacios, personal communication, 2025).

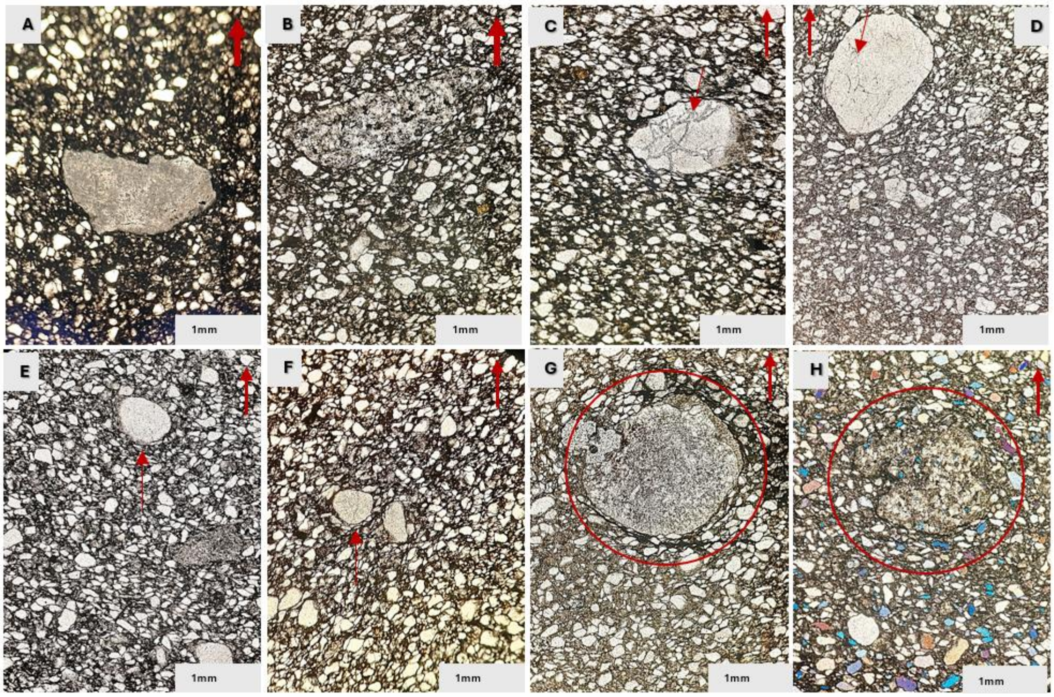

Figure 16. (A) 40x in PPL shows elongated clasts in thin sections with preferred orientation parallel to the bedding (Slide LNM4). (B) 40x in PPL shows elongated clasts in thin sections with preferred orientation parallel to the bedding (Slide UNM7). (C) 40X in PPL shows surficial striation on quartz grains (Slide LNM3). (D) 40X in PPL shows surficial striation on quartz grains (Slide LNM1). (E) 40x in PPL and XPL shows necking structures (Slide UNM8). (F) 40x in PPL and XPL shows necking structures (Slide UNM8). (G) 40x in PPL and XPL shows rotational structures (Slide MNM3). (H) 40x in PPL and XPL shows rotational structures (Slide UNM1). All thin sections are from the Navaldestajo Member, located at CC-432 Navatrasierra geosite. More details in Appendix I

3.2 Quantitative Assessment of Geosites

A quantitative assessment of five geosites, namely, CC-432 Navatrasierra, Las Majuelas, Garganta del Mesto, Arroyo Guadarranquejo, and Charco de la Trucha, was done using the same principles and methods described by Brilha (2016). This methodology distinguishes criteria for four distinct aspects, namely, scientific value (SV), potential educational use (PEU), potential touristic use (PTU), and degradation risk (DR). Each geosite is evaluated using a four-point scale (1-4) rating system, having indicators for each criterion. Each criterion is scored from 1 to 4 points (with zero also being a possibility). The final evaluation of scientific value, degradation risk, educational value, and touristic value of each geosite is derived from the weighted sum of these scores.

Presented herein, the results of the evaluation of geosites within the Villuercas-Ibores-Jara UNESCO Global Geopark for scientific value (Table 3.2), potential educational use (Table 3.4), potential touristic use (Table

3.5), and degradation risk (Table 3.3). These sites were assessed based on multiple criteria (Tables 2.1, 2.3, 2.5 & 2.6). The final values for scientific value, potential educational use, and touristic use were categorized into three classes: <200 (low value), 201-300 (moderate value), and >300(high value) and for degradation risk, <200 (low risk), 201-300 (moderate risk), and >300(high risk).

3.2.1 Scientific Value (SV)

Based on the assessed geosites' results, the final scientific values (Table 8 and Figure 17) fall within the moderate to high categories. CC-432 Navatrasierra is the only geosite with a high scientific value, while the other geosites have moderate scientific values. All the geosites fall under the same framework under consideration, and research has been conducted at the national and international levels (e.g, Doré and Le Gall 1972; Doré 1981; Robardet 1981; Hamouni et al. 1981; Fortuin 1984; Doré et al. 1985; Robardet and Doré 1988), related to the geological element under study. Although representativeness (e.g, CC-432 Navatrasierra), use limitation (e.g, Arroyo Guadarranquejo, due to low fence), and other associated geological features with scientific relevance were the differences between the geosites in the final score, each geosite has excellent preservation of the geological element under study and hence can be used for scientific study. These geosites exhibit a diverse range of geological elements, making them attractive for further studies.

Table 8. Scientific Evaluation of geosites (according to Brilha 2016)

Scientific Value		**Name of geosite**				
Criteria	Weight (Max%)	CC-432 Navatrasierra	Las Majuelas	Garganta del Mesto	Arroyo Guadarranquejo	Charco de la Trucha
Representativeness	120	4x30 = 120	2x30 = 60	2x30 = 60	2x30 = 60	2x30 = 60
Key locality	80	2x20 = 40	2x20 = 40	2x20 = 40	2x20 = 40	2x20 = 40
Scientific Knowledge	20	4x5 = 20	4x5 = 20	4x5 = 20	4x5 = 20	4x5 = 20
Integrity	60	4x15 = 60	4x15 = 60	4x15 = 60	4x15 = 60	4x15 = 60
Geological diversity	20	2x5 = 10	1x5 = 10	1x5 = 10	1x5 = 10	1x5 = 10
Rarity	60	1x 15 = 15	1x15 = 15	1x15 = 15	1x15 = 15	1x15 = 15
Use limitation	40	4x10 = 40	4x10 = 40	4x10 = 40	2x10 = 20	4x10 = 40
Total	**400**	**305**	**245**	**245**	**225**	**245**

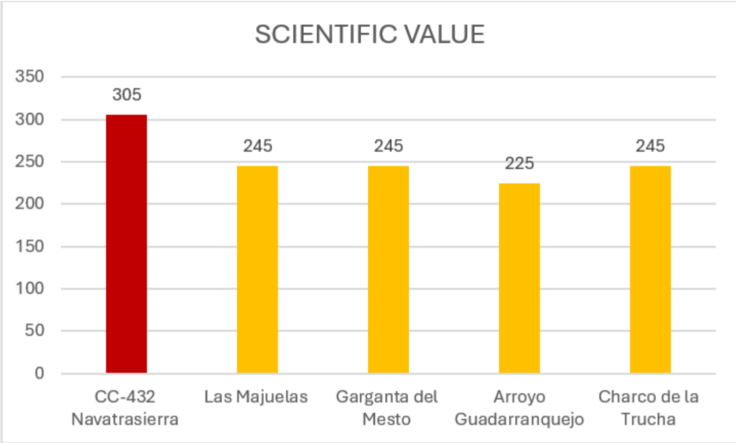

Figure 17. Scientific values of the evaluated geosites, with CC-432 Navatrasierra having the highest value, while other geosites have moderate values.

3.2.2 Degradational Risk (DR)

The assessment of degradation risk based on field observations at these geosites requires particular attention to ensure the safety of visitors and the preservation of the geosites. The degradation risk assessment (Table 9 and Figure 18) shows that CC-432 Navatrasierra, Las Majuelas, and Charco de la Trucha all have low degradation risk, while Garganta del Mesto and Arroyo Guadarranquejo have moderate degradation risk based on the assessment, mainly due to their seasonal variability and locations in river channels. Additionally, natural factors such as weathering and erosion can further degrade these geosites (Garganta del Mesto and Arroyo Guadarranquejo) but also can reveal more geological elements of interest.

Although the geological elements of interest are in excellent condition in each geosite, management should implement restrictions on sampling activities to reduce the risk of degradation of some of these geosites. Continuous monitoring of these geosites can help prevent any further degradation by natural and anthropogenic disturbance.

Table 9. Degradation Risk Evaluation of geosites (according to Brilha 2016)

Degradation Risk		**Name of geosite**				
Criteria	Weight (Max%)	CC-432 Navatrasierra	Las Majuelas	Garganta del Mesto	Arroyo Guadarranquejo	Charco de la Trucha
Deterioration of geological elements	140	1x35 = 35	1x35 = 35	3x35 = 105	3x35 = 105	3x35 = 105
Proximity to areas/activities with potential to cause damage	80	1x20 = 20	0x20 = 0	0x20 = 0	0x20 = 0	0x 20 = 0
Legal protection	80	2x20 = 40	2x20 = 20	2x20 = 40	2x 20 = 40	2x20= 40
Accessibility	60	3x15 = 45	1x15 = 15	3x15 = 45	4x 15 = 60	1x15 = 15
Density of population	40	1x10 =10	1x10 = 10	1x10 = 10	1x10 = 10	1x10 = 10
Total	**400**	**150**	**80**	**200**	**215**	**170**

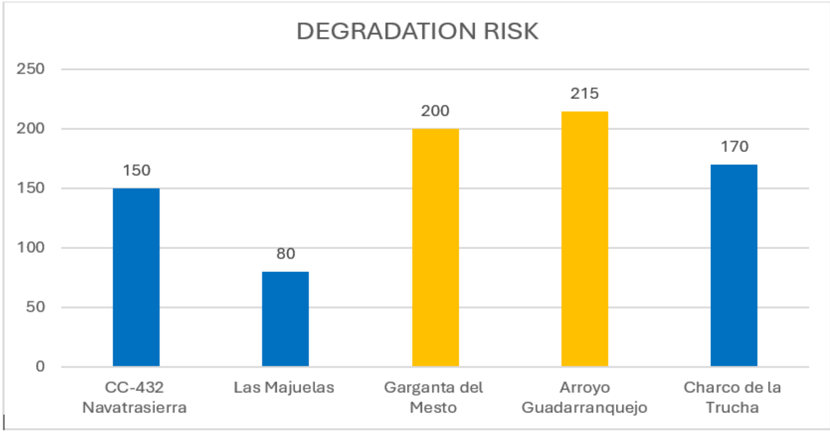

Figure 18. Degradation risk assessments show Garganta del Mesto and Arroyo Guadarranquejo with moderate degradation risk, while other geosites have low degradation risk.

3.2.3 Potential for Educational Use (PEU)

There is a moderate value for potential educational use in all the assessed geosites (Table 10 and Figure 19) except for Las Majuelas, which has low potential educational value. Garganta del Mesto and Arroyo Guadarranquejo geosites are easily accessible, situated along roads, making them convenient for visitors. Their locations make them attractive options for schools seeking educational visits. Charco de la Trucha is accessible via an unpaved road suitable for 4x4 vehicles and is also ideal for educational activities, particularly for university students. However, each site requires infrastructure improvements to enhance safety and provide better protection for visitors and students alike.

Table 10. Potential Educational Use Evaluation of geosites (according to Brilha 2016)

Potential Educational Use		**Name of geosite**				
Criteria	Weight (Max%)	CC-432 Navatrasierra	Las Majuelas	Garganta del Mesto	Arroyo Guadarranquejo	Charco de la Trucha
Vulnerability	40	4x10 = 40	4x10 = 40	4x10 = 40	4x10 = 40	4x10 = 40
Accessibility	40	3x10 = 30	1x10 = 10	2x10 = 20	2x10 = 20	2x10 = 20
Use limitation	20	4x5 = 20	4x5 = 20	4x5 = 20	4x5 = 20	4x5 = 20
Safety	40	2x10 = 20	2x10 = 20	2x10 = 20	2x10 = 20	2x10 = 20
Logistic	20	3x5 = 15	2x5 = 10	2x5 = 10	2x5 = 10	2x5 = 10
Density of population	20	2x5 = 10	2x5 = 10	2x5 = 10	2x5 = 10	2x5 = 10
Association with other values	20	1x5 = 5	1x5 = 5	1x5 = 5	1x5 = 5	1x5 = 5
Scenery	20	0x5 = 0	0x5 = 0	0x5 = 0	0x5 = 0	0x5 = 0
Uniqueness	20	2x5 = 10	2x5 = 10	2x5 = 10	2x5 = 10	2x5 = 10
Observation condition	40	4x10 = 40	2x10 = 20	4x10 = 40	4x10 = 40	4x10 = 40
Didactic potential	80	1x20 = 20	1x20 = 20	1x20 = 20	1x20 = 20	1x20 = 20
Geological diversity	40	3x10 = 30	2x10 = 20	2x10 = 20	2x10 = 20	3x10 = 30
Total	**400**	**240**	**185**	**215**	**215**	**225**

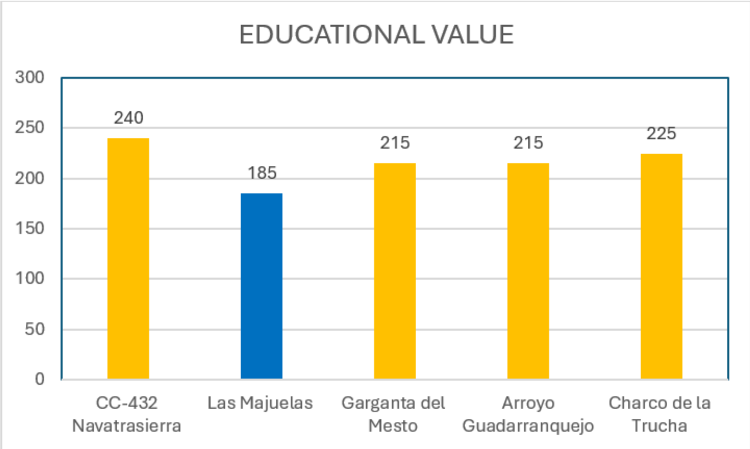

Figure 19. Potential educational use assessment of geosites showed a moderate value across all the geosites except Las Majuelas, which has a low value.

3.2.4 Potential for Touristic Use (PTU)

The potential for touristic use across all the assessed geosites was moderate (Table 11 and Figure 20), except for Las Majuelas, which has low potential. Garganta del Mesto and Arroyo Guadarranquejo geosites are conveniently located along roads and are easily accessible to visitors. Their strategic positions can attract interest from geotourists. Charco de la Trucha can be reached via an unpaved road suitable for 4x4 vehicles and can also serve for tourism due to its stepped waterfall, which could be a major attraction for adventure-loving visitors. This site is especially appealing during the summer because of the scorching temperatures. There is a need for infrastructural development at each of these geosites to enhance safety and visitor protection.

Table 11. Potential Touristic Use Evaluation of geosites (according to Brilha 2016)

Potential Touristic Use		**Name of geosite**				
Criteria	Weight (Max%)	CC-432 Navatrasierra	Las Majuelas	Garganta del Mesto	Arroyo Guadarranquejo	Charco de la Trucha
Vulnerability	40	4x10 = 40	4x10 = 40	4x10 = 40	4x10 = 40	4x10 = 40
Accessibility	40	3x10 = 30	1x10 = 10	2x10 = 20	2x10 = 20	2x10 = 20
Use limitation	20	4x5 = 20	4x5 = 20	4x5 = 20	4x5 = 20	4x5 = 20
Safety	40	2x10 = 20	2x10 = 20	2x10 = 20	2x10 = 20	2x10 = 20
Logistic	20	3x5 = 15	2x5 = 10	2x5 = 10	2x5 = 10	2x5 = 10
Density of population	20	2x5 = 10	2x5 = 10	2x5 = 10	2x5 = 10	2x5 = 10
Association with other values	20	1x5 = 5	1x5 = 5	1x5 = 5	1x5 = 5	1x5 = 5
Scenery	60	0x15 = 0	0x15 = 0	0x15 = 0	0x15 = 0	1x15 = 15
Uniqueness	40	2x10 = 20	2x10 = 20	2x10 = 20	2x10 = 20	2x10 = 20
Observation condition	20	4x5 = 20	2x5 = 10	4x5 = 20	4x5 = 20	4x5 = 20
Interpretative potential	40	3x10 = 30	3x10 = 30	3x10 = 30	3x10 = 30	3x10 = 30
Economic level	20	1x5 = 5	1x5 = 5	1x5 = 5	1x5 = 5	1x5 = 5
Proximity of recreational areas	20	1x5 = 5	1x5 = 5	1x5 = 5	1x5 = 5	1x5 = 5
Total	**400**	**220**	**185**	**205**	**205**	**220**

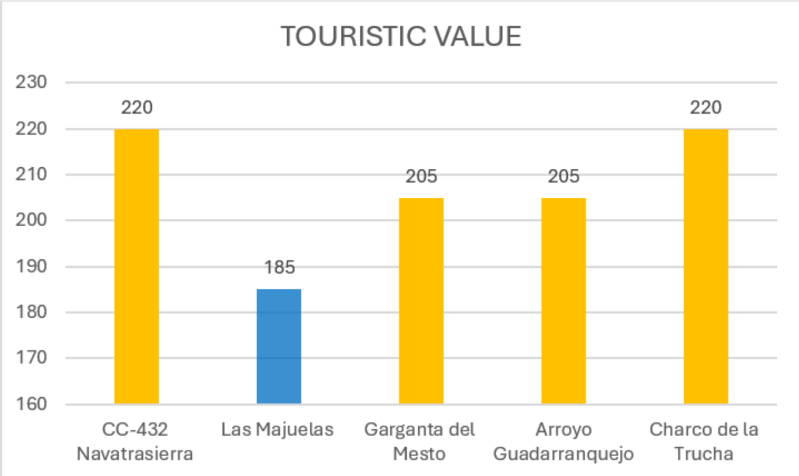

Figure 20. Potential touristic use for all the assessed geosites was moderate, except for Las Majuelas, which has low potential touristic value

Chapter 4: Discussion

4.1 Depositional Environment

The diamictites of Gualija Formation occurred as massive non-stratified rock, although fractures can sometimes resemble bedding planes or be confused as bedding planes and are composed of a dark silt-clay matrix spread in angular to sun-rounded clasts and are characterized by poorly sorted, matrix-supported textures with angular to subrounded grains embedded in a fine-grained silty-clay matrix. This heterogeneous assortment of particles ranges from clay-size grains to centimeters, in which the elongated pebbles tend to show some preferred orientation, commonly with their long dimensions parallel to the bedding. As observed in the thin sections, the presence of micro-deformation structures and surficial striation of clasts indicates a glaciomarine origin.

Diamictites bearing formations in the Iberian Peninsula have been a subject of discussion for several decades whether they resulted from direct glacial activity or secondary mass-wasting processes, with the supporters of glacial origin highlighting evidence of glacial processes such as striated clasts, glaciogenic matric textures, microstructures, and regional correlations with Hirnantian deposits in other part of southwestern Europe and North Africa (e.g Doré and Le Gall 1972; Hammann 1974; Doré 1981; Robardet 1981; Steiner and Falk 1981; Hamouni et al. 1981; Fortuin 1984; Doré et al. 1985; Robardet and Doré 1988; and Rodríguez Nùñez et al. 1989) and some argues that the matrix composition and clast provenance could reflect localized debris flows rather than far-travelled glacial erratic (e.g Greiling (1967)). An ice-rafted mechanism is supported by the presence of dropstones (e.g, Gil Cid et al. 1976; Fortuin

1984; Doré et al. 1985; Robardet and Doré 1988; and Rodríguez-Nùñez et al. 1989), which emphasized marine proximal settings (Paris and Robardet 1977), while subglacial till is suggested due to matrix-dominated textures and flame structures (e.g, Julivert and Truyols 1974), which aligns with the global Hirnantian tillites. With the advancement of knowledge in modern and ancient glacial environments (e.g, Van Der Meer 1993; Menzies 2000; Hiemstra and Rijsdijk 2003; and Menzies et al. 2006; Davies et al. 2011), several criteria allow the recognition of ancient glaciomarine deposits (Hambrey and Harland 1981). Criteria relevant to Gualija diamictites will be discussed to substantiate the evidence of its glaciomarine origin.

Glaciomarine sediments are distinguished from all terrestrial glacial diamictites by the presence of dropstones and marine fossils (Boggs 1995). Glacial sediment load typically consists of an extremely heterogeneous assortment of particles ranging from clay-size grains to meter-size boulders and elongated pebbles tend to show some preferred orientation, commonly with their long dimensions parallel to the bedding (Boggs, 1995), these criteria strongly suggests that the glaciomarine origin of diamictites bearing members of the Gualija Formation in the Guadarranque syncline. The diamictites of the Gualija Formation are characterized by poorly sorted, matrix-supported textures with angular to subrounded grains embedded in a fine-grained silty-clay matrix. This is in accordance with the view of Gil Cid et al. (1976) and Rodríguez-Nùñez et al. (1989). Clast composition suggests recycled lower Paleozoic sedimentary units and basement rocks, while the matrix indicates a prolonged mechanical grinding and pulverizing, likely linked to glacial transport processes. This is in accordance with the observation of Doré and Le Gall (1972) of similar deposits in Normandy.

The occurrence of Gualija diamictites as massive non-stratified rock, even though fractures can sometimes resemble bedding planes, which comprises a dark silt-clay matrix spread in angular to sun-rounded clasts, agrees with the findings of Doré and Le Gall (1972) on the Hirnantian deposits in Normandy. The presence of micro-deformation structures and surficial striation of clasts as observed in the thin sections further indicates glacial influence. The Gualija diamictites correlate broadly with other Hirnantian deposits in the Iberian Peninsula and other places in southwestern Europe (Robardet and Dore 1988); therefore, the depositional setting is very likely to be glaciomarine, correlating with the Hirnantian glaciation.

4.2 Presence of Dropstones

A dropstone is an unusually large or different type of clast introduced vertically or obliquely into host sediment, either singly or in clusters. These can serve as paleoclimatic indicators but require careful interpretation (Bennett and Doyle 1996). Dropstones were observed in the field, despite the absence of distinct lamination in the rock mass that typically aids in their identification. Moreover, the draping of smaller clasts around the larger ones was visible in thin sections.

Mechanisms of transport and entrainment of dropstone could either be by a rafting agent or as a projectile, and four processes of transport and formation were identified by Bennett and Doyle (1996), which include biological rafting, ice rafting, flotation, and projectile. In the context of the current study, only deposition by ice-rafted material seems plausible due to the geographical extent (see below) and age of the sediments.

Donovan and Pickerill (1997), among others, have pointed out an additional possibility of dropstone formation, such as gravity-driven processes (debris flows or turbidites). However, the occurrence of dropstones in the study area, in a poorly sorted diamictite matrix and with no preferred orientations, is consistent with a glaciomarine origin. Moreover, globally acknowledged glaciation during the Hirnantian age provided a paleoenvironmental background that supports the glaciomarine origin of the Gualija Formation. Additionally, the general rarity of fossils and the associated dropstones suggest that environmental stress is consistent with the cold (Yang and Shi 2018). These faunal limitations and the observed microstructures further affirm a glaciomarine origin.

The caution raised by Donovan and Pickerill (1997) of debris flows or turbidites, especially in tectonically active or deeper-marine basins cannot be completely ruled out, but the wider paleoclimatic, stratigraphic setting, the paucity of the faunal context, clasts size, distribution, and orientation of the diamictites in the Gualija Formation all pointed toward ice-rafted origin which at the moment is the most plausible explanation of the diamictites deposits of the Gualija Formation. This interpretation is consistent with the criteria established by Bennett and Doyle (1996).

4.3 Geographical extent and stratigraphic correlation

Wide geographical extent is another important criterion pointed out by Bennett and Doyle (1996), as icebergs have the potential to transport dropstones over large areas. The fact that the Guadarranque Syncline (with diamictite deposits) extends over 100 km in the Central-Iberian zone (Rodríguez-Núñez et al. 1989) reinforces this point. These deposits are not isolated but are part of the regionally consistent depositional event as interpreted in many localities as glaciomarine in origin. These sediments have been correlated with other parts of Spain, Portugal, France, and Germany by Robardet & Doré (1988) where they concluded that in all regions, the diamictite formations are made up of related lithologies regarding their origin and composition.

In Spain, Fortuin (1984) discusses the depositional environment and characteristics of the Orea Shale Formation in the Sierra de Albarracin region of southeastern Spain and concludes that the Orea Shale Formation is of glaciomarine origin. In Portugal, Young (1985 and 1988), during the revision of the upper Ordovician stratigraphy of Buçaco Syncline, Central Portugal, confirmed that the Casal Carvalhal Formation, which stratigraphically correlated with the Gualija Formation, was indeed of glaciomarine origin. Furthermore, Colmenar et al. (2019) concurred with this view. In Thuringia (Germany), Steiner and Falk (1981) interpreted the diamictite-like units as Hirnantian glacial deposits. Additionally, Doré (1981) and Doré et al. (1985) interpreted the Upper Ordovician diamictite deposits as having angular clasts in a fine-grained matrix, suggesting their origin as glaciomarine.

Despite the limited availability of fossil content in the Gualija Formation, lithostratigraphic correlation with other formations of the same age in southwestern Europe confirmed its Hirnantian age and thus supports its glaciomarine origin. Additionally, sedimentological and palaeontological evidence from these regions supports the glaciomarine influence of these deposits. Moreover, Colmenar et al. (2019) agree with the view of Young (1988) on the glaciomarine origin of Casal Carvalhal Formation, in the Buçaco Syncline, in central Portugal, which is stratigraphically comparable to Gualija Formation. These deposits are believed to be of glaciomarine origin, with the isolated pebbles interpreted as dropstones. These sediments are closely comparable with those of similar age in other parts of Iberia and Armorica (e.g., the "Pélites à fragments" of Normandy).

4.4 Geosites evaluation

A geosite is understood as a remarkable geological locality where one or more elements of geodiversity are present and unique values of scientific, pedagogical, cultural, or touristic interest are shown (Brilha 2005); therefore, an inventory of geosites is crucial to understanding the concept of geoconservation. Over the last decades, geoconservation (Sharples et al. 2002) approaches have become very popular, contributing significantly as an important component of nature conservation practices (Prosser et al. 2013). Degradation of the environment driven by the constantly increasing human pressure on our planet has made clear the need to record, protect, and promote not only biodiversity but geodiversity as well (Gray 2013).

Preserving geological heritage has thus become a key factor for future legislation and policies that would allow a more effective management of the natural environment through the protection of geosites (Gordon et al., 2018). To achieve these goals, geosite conservation practices need to be implemented to limit human and natural deterioration or destruction (Prosser et al. 2018). Nevertheless, to plan or take specific geoconservation measures for geosites and particularly in places where geoconservation can be enhanced, such as geoparks, geosite assessments need to be implemented first to identify their value, possible threats, and the need for protection (Prosser et al. 2018; Crofts et al. 2020). Except for geoconservation, geoparks in their effort to promote sustainable development and economic benefits for local communities through geotourism and education, have also as main goals, the connection of nature with people and the connection of geodiversity with biodiversity, cultural heritage, and local communities (Gordon et al. 2018; Gordon 2019; Farsani et al. 2014). Through geotouristic and educational activities organised by the geoparks, geoscientific knowledge and geoconservation concepts are transferred to the public (Farsani et al. 2014)

Based on the results in chapter 3 above, the study area has a rich diamictite geoheritage sites that hold significance for scientific research and potential for developing geo-education and possibly geotourism. Among the identified locations, the CC-432 Navatrasierra stands out as the geosite with the highest potential for scientific value due to its easy access, completeness, and association with other geodiversity elements. Nonetheless, all the remaining evaluated geosites show moderate scientific value. It is also worth noting that all the evaluated geosites have moderate educational and touristic values except Las Majuelas, mainly due to the lack of educational and touristic infrastructures. CC-432 Navatrasierra should be used for scientific purposes only due to its location on the roadside with no protection. Providing the educational and touristic infrastructures in some of these geosites will increase their touristic appeal and educational value from moderate to possibly very high. Addition of these geosites to the current list of geosites in the geopark will increase the diversity of geological elements within the geopark and strengthen its global recognition for their significant scientific value, educational value, and potential for touristic use. It is recommended that the CC-432 Navatrasierra geosite should only be used for scientific purposes due to safety concerns. It cannot be used for educational or touristic purposes, as that will endanger students or tourists due to the moving vehicles. Equally important, Garganta del Mesto, Charco de la Trucha, and Arroyo Guadarranquejo should be used for touristic and educational purposes, taking into account the seasonal visibility of the geological elements of interest.

5.0 Chapter Five: Conclusion

(1) The late Ordovician deposits (Gualija Formation) contain three members exhibiting stratigraphic disparity, reaching a thickness of up to 144 meters. The Risquillo and Navaldestajo members contain diamictite with particle sizes ranging from less than millimeters to centimeters and are dark gray to black, and sometimes medium gray (when weathered). They are poorly sorted and vary from angular to

subrounded as observed in the field, and are unstratified and often lack clear bedding planes over significant thicknesses (5–10 m), although fractures can sometimes resemble bedding planes.

(2) In thin sections, both the Risquillo Member and the Navaldestajo Member consist of poorly sorted, silty/clay matrix diamictites with no overall preferred orientation of the grains, as they are rather oriented in a random manner throughout. However, the elongated clasts tend to show preferred orientation, commonly with their long dimensions parallel to the bedding. Additionally, grain surface textures are generally rough, with fractures in some cases, and surficial striations. The chaotic fragment distributions contain angular to subrounded clasts of less than 1 millimeter as observed in thin sections embedded in a fine-grained silty-clay matrix, to a few millimeters. The composition of diamictite-bearing members of the Gualija Formation is likely to be derived from the basement rocks, volcanic rocks, and recycled older sedimentary rocks. Microstructures include necking, rotational structures, and surficial striations on quartz grains. There is a general rarity of both trace and body fossils in the Gualija Formation, as acritarch analysis yielded a negative result.

(3) The presence of dropstones in the study area, as observed in the field, and the draping of smaller clasts around the larger ones as observed in thin sections strongly suggested deposition of these sediments by ice-rafting, which geographical extent further supported. Additionally, globally acknowledged glaciation during the Hirnantian age provided a paleoenvironmental background that supports the glaciomarine origin of the Gualija Formation. Furthermore, the general rarity of fossils and the associated dropstones suggests environmental stress, which is consistent with the cold, as Yang and Shi (2018) pointed out. These faunal limitations, along with the observed microstructures, further affirm a glaciomarine origin.

(4) The Gualija diamictites correlate broadly with other Hirnantian deposits in the Iberian Peninsula and other places in southwestern Europe, where the depositional settings were all interpreted as glaciomarine, correlating with the Hirnantian glaciation.

(5) A quantitative assessment of five geosites, namely, CC-432 Navatrasierra, Las Majuelas, Garganta del Mesto, Arroyo Guadarranquejo, and Charco de la Trucha, was done using the same principles and methods described by Brilha (2016). The result of the evaluation of geosites for scientific value, potential educational use, potential touristic use, and degradation risk was based on multiple criteria. The final values for scientific value, potential educational use, and touristic use were categorized into three classes: <200 (low value), 201-300 (moderate value), and >300(high value) and for degradation risk, <200 (low risk), 201-300 (moderate risk), and >300(high risk).

(6) Based on the results of scientific value, touristic value, and educational value, the study area has a significant geological heritage based on the presence of diamictites. Geosites hold significance for scientific research and potential for developing geo-education and possibly geotourism. Among the identified locations, the CC-432 Navatrasierra stands out as the geosite with the highest potential for scientific value due to its easy access, completeness, and association with other geodiversity elements. Nevertheless, all the evaluated geosites show moderate scientific value. Equally important, all the evaluated geosites have moderate educational and touristic values except Las Majuelas. Many of these geosites can attain a higher score than the current one if educational and touristic infrastructures are developed. Therefore, providing the educational and touristic infrastructures in some of these geosites will increase their touristic appeal and educational value from moderate to possibly very high. The provision of these infrastructures will require further research to reevaluate these geosites to reflect their significance. Degradation risk was generally low except for Garganta del Mesto and Arroyo Guadarranquejo, possibly due to their location in seasonal river channels.

In conclusion, the addition of these geosites to the current list of geosites in the geopark will increase the diversity of geological elements within the geopark and strengthen its global recognition for their significant scientific value, educational value, and potential for educational use.

References

Álvaro, J. J., Cortijo, I., Jensen, S., Lorenzo, S., and Pieren, A. P. (2019). Updated stratigraphic framework and biota of the Ediacaran and Terreneuvian in the Alcudia-Toledo Mountains of the Central Iberian Zone, Spain. Estudios Geológicos, 75(2), e093. https://doi.org/10.3989/egeol.43620.548

Bennett, M. R. and Doyle, P. (1996). Dropstones: their origin and significance. Palaeogeography, Palaeoclimatology, Palaeoecology, 126(1-2), 83–98. doi:10.1016/0031-0182(95)00093-0

Boggs, S Jr. (1995). Principles of Sedimentology and Stratigraphy. (2nd ed.). Prentice Hall.

Brenchley, P.J., Marshall, J.D., Carden, G.A.F., Robertson, D.B.R., Long, D.G.F., Meidla, T., Hints, L., and Anderson, T.F. (1994). Bathymetric and isotopic evidence for the short-lived Late Ordovician glaciation in a greenhouse period: Geology, v 22, 295-298.

Brilha, J. B. R. (2005). Património geológico e geoconservação: a conservação da natureza na sua vertente geológica. Viseu: Palimage Editores. 190 p. ISBN 972-8575-90-4

Brilha, J. B. R. (2016). Inventory and Quantitative Assessment of Geosites and Geodiversity Sites: A Review. Geoheritage 8, 119–134. https://doi.org/10.1007/s12371-014-0139-3.

Carls, P. (1975). The Ordovician of the Eastern Iberian Chains near Fombuena and Luesma (Prov. Zaragoza, Spain). Neues Jahrbuch für Geologie und Paläontologie - Abhandlungen, 150(2), 127–146.

Colmenar, J., Pereira, S., Young, T. P., da Silva, C. M., and Sá, A. A. (2019). First report of Hirnantian (Upper Ordovician) high-latitude peri-Gondwanan macrofossil assemblages from Portugal. Journal of Paleontology, 93(3), 460–475. https://doi.org/10.1017/jpa.2018.88

Cortijo, I.; Martí Mus, M.; Jensen, S. and Palacios, T. (2010). A new species of Cloudina from the terminal Ediacaran of Spain. Precambrian Research, 176, 1–10. https://doi.org/10.1016/j.precamres.2009.10.010

Cortijo, I.; Martí Mus, M.; Jensen, S. and Palacios, T. (2015). Late Ediacaran skeletal body fossil assemblage from the Navalpino anticline, central Spain. Precambrian Research, 267, 186–195. https://doi.org/10.1016/j.precamres.2015.06.013

Crofts, R., Gordon, J. E., Brilha, J., Gray, M., Gunn, J., Larwood, J., Santucci, V., Tormey, D., & Worboys, G. L. (2020). Guidelines for geoconservation in protected and conserved areas (C. Groves, Ed.). International Union for Conservation of Nature (IUCN). https://doi.org/10.2305/IUCN.CH.2020.PAG.31.en

Davies, B. J., Roberts, D. H., Bridgland, D. R., Ó Cofaigh, C., Riding, J. B., Demarchi, B., Penkman, K., and Pawley, S. M. (2012). Timing and depositional environments of a Middle Pleistocene glaciation of northeast England: New evidence from Warren House Gill, County Durham. Quaternary Science Reviews, 44, 180–212.

Destombes, J. (1968). Sur la nature glaciaire des sédiments du groupe du 2e Bani, Ashgill supérieur de l'Anti-Atlas (Maroc). Comptes Rendus de l'Académie des Sciences, Série D, 267, 684–686.

Destombes, J. (1981). Hirnantian (Upper Ordovician) tillites on the north flank of the Tindouf Basin, Anti-Atlas, Morocco. In M. Hambrey & W. Harland (Eds.), Earth's Pre-Pleistocene Glacial Record (pp. 84–88). Cambridge University Press.

Destombes, J., Hollard, H., and Willefert, S. (1985). Lower Palaeozoic rocks of Morocco. In C. H. Holland (Ed.), Lower Paleozoic of North-Western and West-Central Africa (pp. 91–336). Wiley.

Donovan, S. K., and Pickerill, R. K. (1997). Dropstones: Their origin and significance: A comment. Palaeogeography, Palaeoclimatology, Palaeoecology, 131(1–2), 175–178. https://doi.org/10.1016/S0031-0182(96)00150-2

Doré, F. (1981). The late Ordovician tillite in Normandy (Armorican Massif). In M. Hambrey & W. Harland (Eds.), Earth's Pre-Pleistocene Glacial Record (pp. 582–584). Cambridge University Press.

Doré, F., and Le Gall, J. (1972). Sedimentologie de la tillite de Feuguerolles (Ordovicien supérieur de Normandie). Bulletin de la Société Géologique de France, 14, 199–211.

Doré, F., Dupret, L., and Le Gall, J. (1985). Tillites et tilloides du Massif Armoricain. Palaeogeography, Palaeoclimatology, Palaeoecology, 51, 85–96.

Eyles, N. (2008). Glacio-epochs and the supercontinent cycle after ∼3.0 Ga: Tectonic boundary conditions for glaciation. Palaeogeography, Palaeoclimatology, Palaeoecology, 258, 89–129. https://doi.org/10.1016/j.palaeo.2007.09.021

Farsani, N. T., Coelho, C. O. A., Costa, C. M. M., and Amrikazemi, A. (2014). Geo-Knowledge management and geoconservation via geoparks and geotourism. Geoheritage, 6, 185–192.

Fernández Álvarez, R. (2020). Geoparks and Education: UNESCO Global Geopark Villuercas-Ibores-Jara as a Case Study in Spain. Geosciences, 10(1), 27. https://doi.org/10.3390/geosciences10010027

Finlay, A. J., Selby, D., and Gröcke, D. R. (2010). Tracking the Hirnantian glaciation using Os isotopes. Earth and Planetary Science Letters, 293(3–4), 339–348. https://doi.org/10.1016/j.epsl.2010.02.049

Finnegan, S., Bergmann, K., Eiler, J. M., Jones, D. S., Fike, D. A., Eisenman, I., Hughes, N. C., Tripati, A. K., and Fischer, W. W. (2011). The magnitude and duration of late Ordovician–early Silurian glaciation. Science, 331(6024), 903–906. https://doi.org/10.1126/science.1200803

Folk, R. L. (1951). Petrology of sedimentary rocks. Hemphill Publishing Company

Fortuin, A. R. (1984). Late Ordovician glaciomarine deposits (Orea Shale) in the Sierra de Albarracín, Spain. Palaeogeography, Palaeoclimatology, Palaeoecology, 48(3–4), 245–261. https://doi.org/10.1016/0031-0182(84)90047-6

Ghienne, J.-F. (2003). Late Ordovician sedimentary environments, glacial cycles, and post-glacial transgression in the Taoudeni Basin, West Africa. Palaeogeography, Palaeoclimatology, Palaeoecology, 189(1–2), 117–145. https://doi.org/10.1016/S0031-0182(02)00694-6

Ghienne, J.-F., Le Heron, D. P., Moreau, J., Denis, M., and Deynoux, M. (2007). The late Ordovician glacial sedimentary system of the North Gondwana Platform. In J. A. Hambrey, P. F. Barker, & A. J. S. L. Whitham (Eds.), Glacial sedimentary processes and products (pp. 295–319). Wiley. https://doi.org/10.1002/9781444304435.ch17

Gil Cid, M. D., Gutiérrez Elorza, M., Romariz, C., and Vegas, R. (1976). El Ordovícico y Silúrico del sinclinal de Guadarranque–Gualija (Prov. de Cáceres, España). Comunicaciones del Servicio Geológico de Portugal, 60, 17–31.

Gordon, J. E. (2019). Geoconservation principles and protected area management. International Journal of Geoheritage Parks, 7(3), 199–210. https://doi.org/10.1016/j.ijgeop.2019.07.001

Gordon, E. J., Crofts, R., and Díaz-Martínez, E. (2018). Geoheritage conservation and environmental policies. In Geoheritage (pp. 213–235). Elsevier.

Gray, M. (2013). Geodiversity: Valuing and conserving abiotic nature (2nd ed.). Wiley.

Greiling, L. (1967). Der Thüringische Lederschiefer. Geologie und Paläontologie, 1, 3–11.

Gutiérrez-Marco, J. C., Piçarra, J. M., Meireles, C. A., Cózar, P., García-Bellido, D. C., Pereira, Z., Vaz, N., Pereira, S., Lopes, G., Oliveira, J. T., Quesada, C., Zamora, S., Esteve, J., Colmenar, J., Bernárdez, E., Coronado, I., Lorenzo, S., Sá, A. A., Dias Da Silva, Í., ... Gómez-Barreiro, J. (2019). Early Ordovician–Devonian passive margin stage in the Gondwanan units of the Iberian Massif. In C. Quesada & J. T. Oliveira (Eds.), The geology of Iberia: A geodynamic approach (pp. 75–98). Springer. https://doi.org/10.1007/978-3-030-10519-8_3

Hammann, W. (1974). Die ordovizisch-silurische Grenzschichten in Thüringen (DDR). Zeitschrift für geologische Wissenschaften, 9(3), 337–348.

Hamoumi, N., Le Ribault, L., and Pelhate, A. (1981). Les Schistes du Cosquer (Ordovicien supérieur, Massif armoricain occidental): Une formation glacio-marine à la périphérie d'un inlandsis ordovicien. Bulletin de la Société Géologique de France, 7(22), 279–286.

Hambrey, M. J., and Harland, W. B. (Eds.) (1981). Earth's pre-Pleistocene glacial record. Cambridge University Press. https://doi.org/10.1017/CBO9780511564193

Harper, D. A. T., Hammarlund, E. U., and Rasmussen, C. M. Ø. (2014). End Ordovician extinctions: A coincidence of causes. Gondwana Research, 25(6), 1294–1307. https://doi.org/10.1016/j.gr.2013.12.013

Hiemstra, J. F., and Rijsdijk, K. F. (2003). Observing artificially induced strain: Implications for subglacial deformation. Journal of Quaternary Science, 18(4), 373–383. https://doi.org/10.1002/jqs.769

Jin, C. S., Liao, Z. W., and Lash, G. G. (2021). High-frequency redox variation across the Ordovician–Silurian transition, South China. Palaeogeography, Palaeoclimatology, Palaeoecology, 566, 110218. https://doi.org/10.1016/j.palaeo.2021.110218

Julivert, M. and Truyols, J. (1974). Nuevos datos sobre el Ordovícico del sinclinal de Guadarranque (Cáceres). Breviora Geológica Asturica, 18(4), 57–61.

Kump, L. R., Arthur, M. A., Patzkowsky, M. E., Gibbs, M. T., Pinkus, D. S., and Sheehan, P. M. (1999). A weathering hypothesis for glaciation at high atmospheric pCO2 during the Late Ordovician: Interpreting carbon-isotope excursions: Carbonates and organic matter. Palaeogeography, Palaeoclimatology, Palaeoecology, 152(1-2), 181–198. https://doi.org/10.1016/S0031-0182(99)00066-3

Le Heron, D. P., Sutcliffe, O., Bourgig, K., Craig, J., Visentin, C., and Whittington, R. (2004). Sedimentary architecture of Upper Ordovician tunnel valleys, Gargaf Arch, Libya: Implications for the genesis of a hydrocarbon reservoir. GeoArabia, 9(2), 137–160.

Le Heron, D. P., and Craig, J. (2008). First-order reconstructions of a Late Ordovician Saharan ice sheet. Journal of the Geological Society, 165(1), 19–29. https://doi.org/10.1144/0016-76492007-002

Lenton, T. M., Crouch, M., Johnson, M., Pires, N., & Dolan, L. (2012). The first plants cooled the Ordovician. Nature Geoscience, 5(2), 86–89. https://doi.org/10.1038/ngeo1376

Lewin, A., Meinhold, G., Hinderer, M., Dawit, E. L., & Bussert, R. (2018). Provenance of sandstones in Ethiopia during Late Ordovician and Carboniferous–Permian Gondwana glaciations: Petrography and geochemistry of the Enticho Sandstone and the Edaga Arbi Glacials. Sedimentary Geology, 375, 188–202. https://doi.org/10.1016/j.sedgeo.2017.10.006

Lima, F. F., Brilha, J., and Salamuni, E. (2010). Inventorying geological heritage in large territories: A methodological proposal applied to Brazil. Geoheritage, 2(3-4), 91–99. https://doi.org/10.1007/s12371-010-0017-5

Linnemann, U., Pieren, A., Hofmann, M., Drost, K., Quesada, C., Gärtner, A., Zieger, J., and Ullrich, J. (2018). A ~565 Ma old glaciation in the Ediacaran of peri-Gondwanan West Africa. International Journal of Earth Sciences, 107(3), 885–911. https://doi.org/10.1007/s00531-017-1520-7

Melchin, M. J., Mitchell, C. E., Holmden, C., and Štorch, P. (2013). Environmental changes in the Late Ordovician–early Silurian: Review and new insights from black shales and nitrogen isotopes. Geological Society of America Bulletin, 125(11-12), 1635–1670. https://doi.org/10.1130/B30843.1

Menzies, J. (2000). Micromorphological analyses of microfabrics and microstructures indicative of deformation processes in glacial sediments. In A. J. Maltman, A. J. Hubbard, and M. J. Hambrey (Eds.), Deformation of glacial materials (Vol. 176, pp. 245–257). Geological Society of London.

Menzies, J., van der Meer, J. J. M., and Rose, J. (2006). Till—as a glacial "tectomict," its internal architecture, and the development of a "typing" method for till differentiation. Geomorphology, 75(1-2), 172–200. https://doi.org/10.1016/j.geomorph.2005.07.007

Moreno Serrano, F. (1974). Las formaciones anteordovícicas del anticlinorio anal de Valdelacasa. Boletín Geológico y Minero de España, 85, 396–400.

Paris, F., and Robardet, M. (1977). Paléogéographie et relations ibéro-armoricaines au Paléozoïque anté-Carbonifère. Bulletin de la Société Géologique de France, Série 7, 19, 1121–1126.

Pieren Pidal, A. P. (2000). Las sucesiones anteordovícicas de la región oriental de la provincia de Badajoz y área contigua de la de Ciudad Real (PhD thesis, Complutense University, Madrid). http://eprints.ucm.es/5512/

Pogge Von Strandmann, P. A. E., Desrochers, A., Murphy, M. J., Finlay, A. J., Selby, D., and Lenton, T. M. (2017). Global climate stabilisation by chemical weathering during the Hirnantian glaciation. Geochemical Perspectives, 3, 230–237.

Prosser, C. D., Díaz-Martínez, E., and Larwood, J. G. (2019). The conservation of geosites. In Geoheritage (pp. 193–212). Elsevier.

Pulido Fernández, T., & Marín, R. G. (2014). Geosites inventory in the Geopark Villuercas-Ibores-Jara (Extremadura, Spain): A proposal for a new classification. Geoheritage, 6(1), 17–27. https://doi.org/10.1007/s12371-013-0088-2

Robardet, M. (1981). Late Ordovician tillites in the Iberian Peninsula. In M. Hambrey & W. Harland (Eds.), Earth's Pre-Pleistocene Glacial Record (pp. 585–589). Cambridge University Press.

Robardet, M., and Doré, F. (1988). The late Ordovician diamictic formations from southwestern Europe: North-Gondwana glaciomarine deposits. Palaeogeography, Palaeoclimatology, Palaeoecology, 66(1–2), 19–31. https://doi.org/10.1016/0031-0182(88)90078-8

Robardet, M., and Gutiérrez-Marco, J. C. (2004). The Ordovician, Silurian, and Devonian sedimentary rocks of the Ossa-Morena Zone (SW Iberian Peninsula, Spain). Journal of Iberian Geology 30 (2004) 73-92).

Robardet, M., Vegas, R., and Paris, F. (1980). El techo del Ordovícico en el centro de la Península Ibérica. Studia Geologica Salmanticensia, 16, 103–121.

Rodríguez-Núñez, J., Gutierrez-Marco, J.C. and Sarmiento, G. (1989). Rasgos bioestratigráficos de la sucesión silúrica del Sinclinal del Guadarranque (Zona Centroibérica, España). Cuadernos do Laboratorio Xeolóxico de Laxe, 14, 129–148.

Saltzman, M. R., and Young, S. A. (2005). Long-lived glaciation in the Late Ordovician? Isotopic and sequence-stratigraphic evidence from western Laurentia. Geology, 33(2), 109–112. https://doi.org/10.1130/G21219.1

Sharples, C. (2002). Concepts and principles of geoconservation. Tasmanian Parks & Wildlife Service.

Prosser, C. D., Brown, E. J., Larwood, J. G., and Bridgland, D. R. (2013). Geoconservation for science and society—An agenda for the future. Proceedings of the Geologists' Association, 124(4), 561–567.

Sproson, A. D., von Strandmann, P. A. E., Selby, D., Jarochowska, E., Frýda, J., Hladil, J., Loydell, D. K., Slavík, L., Calner, M., Maier, G., et al. (2022). Osmium and lithium isotope evidence for weathering feedbacks linked to orbitally paced organic carbon burial and Silurian glaciations. Earth and Planetary Science Letters, 577, 117260.

Steiner, J., and Falk, F. (1981). The Ordovician Lederschiefer of Thuringia. In M. Hambrey & W. Harland (Eds.), Earth's Pre-Pleistocene Glacial Record (pp. 579–581). Cambridge University Press.

Sutcliffe, O. E., Dowdeswell, J. A., Whittington, R. J., Theron, J. N., and Craig, J. (2000). Calibrating the Late Ordovician glaciation and mass extinction by the eccentricity cycles of Earth's orbit. Geology, 28(10), 967–970. https://doi.org/10.1130/0091-7613(2000)28<967:CTLOGA>2.0.CO;2

Swanson-Hysell, N. L., and Macdonald, F. A. (2017). Tropical weathering of the Taconic Orogeny as a driver for Ordovician cooling. Geology, 45(8), 719–722. https://doi.org/10.1130/G38982.1

Tang, P., Yang, X., and Yan, D. (2024). Enhanced continental weathering triggered the anoxia of seawater and mass extinctions during the Late Ordovician. Journal of Marine Science and Engineering, 12(12), 2237. https://doi.org/10.3390/jmse12122237

Torsvik, T. H., and Cocks, L. R. M. (2017). Earth history and palaeogeography (101-123 pp.). Cambridge University Press. https://doi.org/10.1017/9781316225523

Torsvik, T. H., and Cocks, L. R. M. (2013). Gondwana from top to base in space and time. Gondwana Research, 24(4), 999–1030. https://doi.org/10.1016/j.gr.2013.06.012

UNESCO Global Geopark Villuercas-Ibores-Jara. (2019). Situation map, Geological map, and geosites. Retrieved May 25, 2019, from https://www.geoparquevilluercas.es/?lang=en

Van der Meer, J. J. M. (1993). Microscopic evidence of subglacial deformation. Quaternary Science Reviews, 16(8), 827–831. https://doi.org/10.1016/0277-3791(93)90056-K

Yang, B., and Shi, G. R. (2018). Co-occurrence patterns of ice-rafted dropstones and brachiopods from a Late Paleozoic glaciomarine succession in the Itararé Group, Brazil: Implications for habitat disturbances. Journal of the Geological Society, 175(5), 813–824. https://doi.org/10.1144/jgs2017-155

Young, T. P. (1985). The stratigraphy of the Upper Ordovician of central Portugal (Unpublished doctoral thesis). University of Sheffield, Sheffield, UK.

Young, T. P. (1988). The lithostratigraphy of the upper Ordovician of central Portugal. Journal of the Geological Society, 145(3), 377–392. https://doi.org/10.1144/gsjgs.145.3.0377

Appendix I

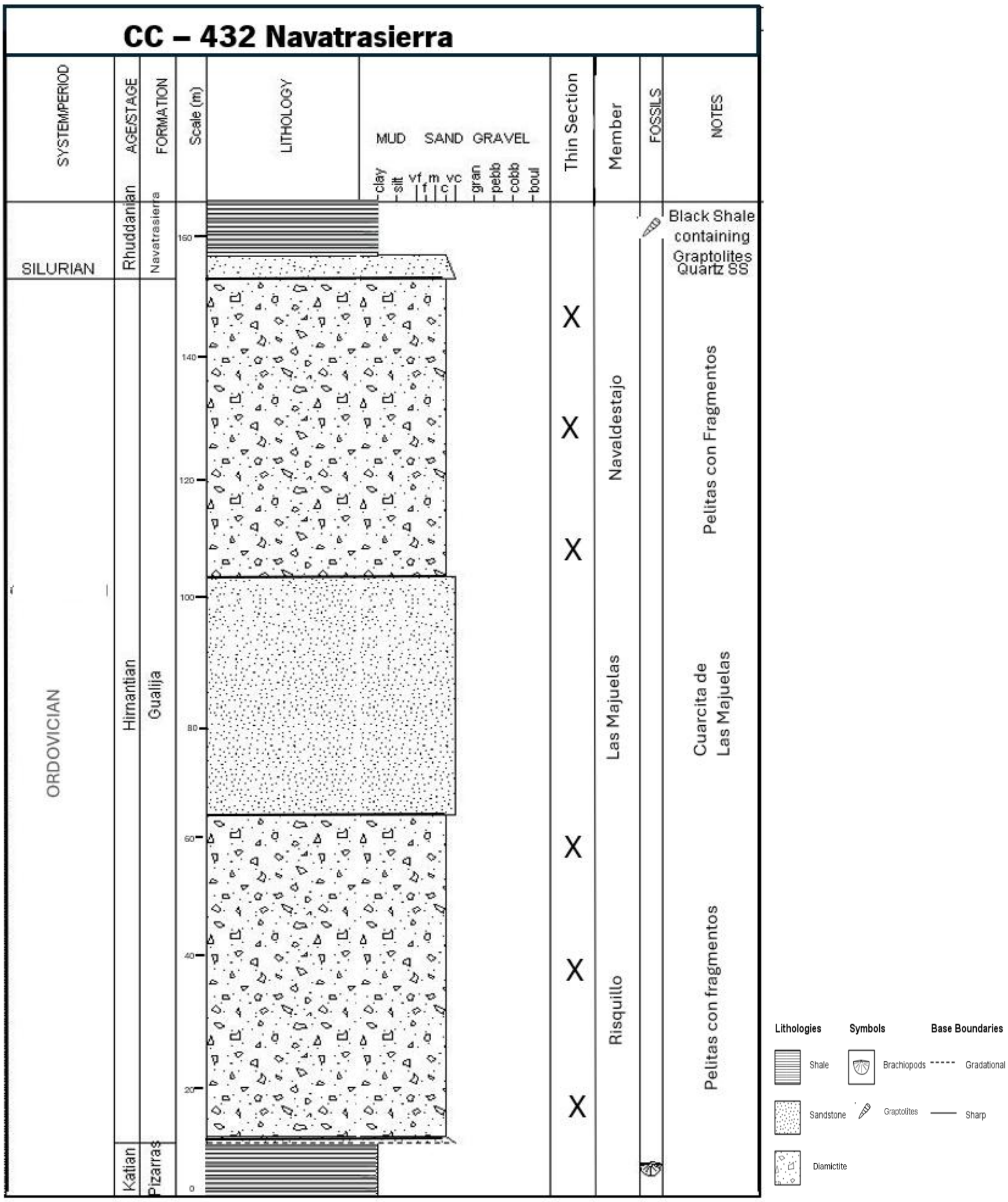

Figure 1. Stratigraphic log of CC-432 Navatrasierra showing where samples for the thin sections were taken from.

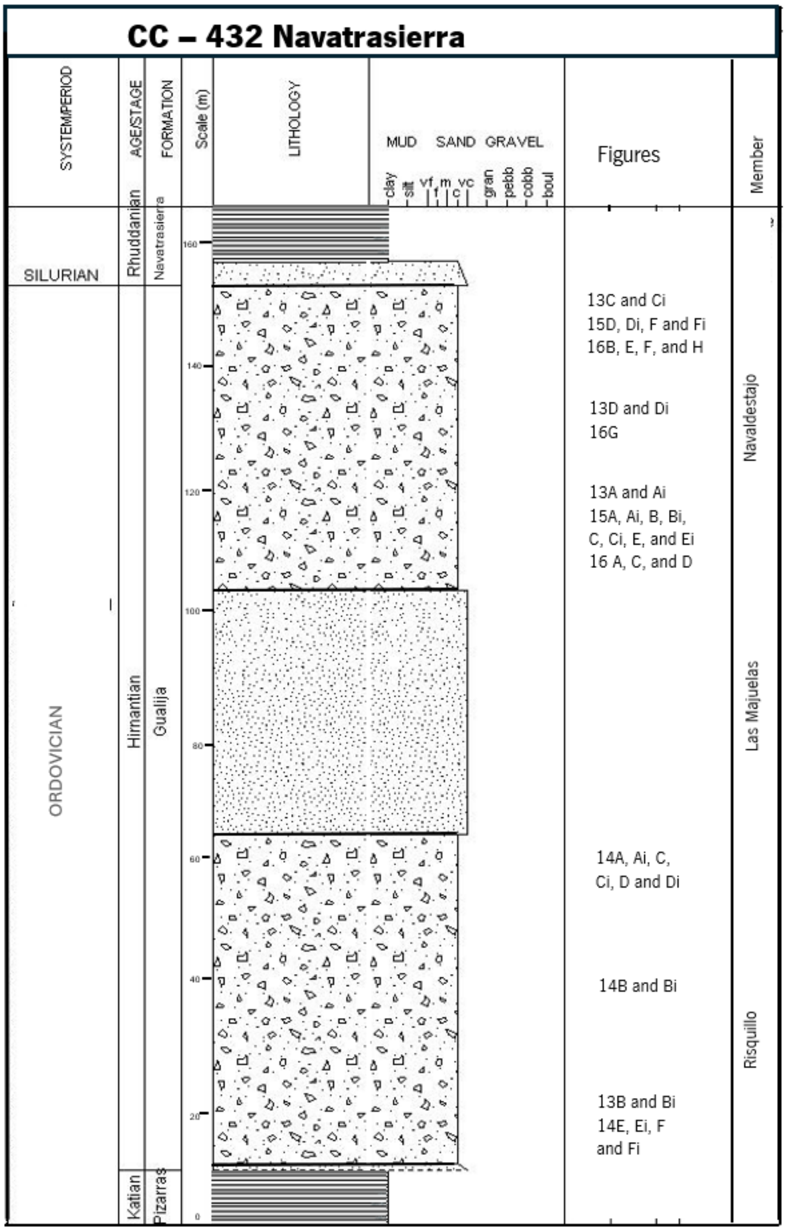

Figure 2. Stratigraphic log of CC-432 Navatrasierra showing the provenance of the thin sections.